



## Durham E-Theses

---

### *Negative regulation of Ire1 during the unfolded protein response*

READ, ADAM

#### How to cite:

---

READ, ADAM (2022) *Negative regulation of Ire1 during the unfolded protein response*, Durham theses, Durham University. Available at Durham E-Theses Online: <http://etheses.dur.ac.uk/14672/>

#### Use policy

---

The full-text may be used and/or reproduced, and given to third parties in any format or medium, without prior permission or charge, for personal research or study, educational, or not-for-profit purposes provided that:

- a full bibliographic reference is made to the original source
- a [link](#) is made to the metadata record in Durham E-Theses
- the full-text is not changed in any way

The full-text must not be sold in any format or medium without the formal permission of the copyright holders.

Please consult the [full Durham E-Theses policy](#) for further details.

# **Masters by Research (M.Res) Thesis**

Durham University, Department of Biosciences, Durham DH1 3LE, United Kingdom.

## **Negative regulation of Ire1 during the unfolded protein response**

**Student:** Mr Adam M. Read

**Supervisor:** Dr Martin Schröder

Wednesday 30<sup>th</sup> March 2022

## 1.0 Abstract

When cells undergo endoplasmic reticulum stress due to a build-up of unfolded or misfolded proteins, the cell must adapt to this stress and does so through the unfolded protein response (UPR). Ire1, a protein kinase endoribonuclease, is a protein found in the endoplasmic reticulum (ER) of *Saccharomyces cerevisiae* and plays a major role in the cell's adaptive response to ER stress. Upon accumulation of unfolded proteins in the ER, Ire1 becomes active and splices *HAC1* mRNA. After splicing the *HAC1* mRNA is translated to produce the Hac1<sup>i</sup> protein, the Hac1<sup>i</sup> protein contains a bZIP transcription factor which leads to alleviation of ER stress by promoting inducing expression of UPR-associated genes. Previous work has shown that although phosphorylation is not essential to RNase activation, it still plays a critical role. Therefore, this study investigates previously identified phosphatases, Dcr2 and Ptc2, which were proposed to be negative regulators of Ire1. This study shows that out of the two investigated phosphatases, only Ptc2 was observed to negatively regulate the UPR. The mechanism of activation for the way in which the UPR was inactivated determined that interference of IRE1 clustering was affected by overexpression of either phosphatase, which suggests an alternative mechanism.

## Table of Contents

<b>1.0 Abstract</b> .....	<b>2</b>
<b>2.0 Acknowledgments</b> .....	<b>4</b>
<b>3.0 Statement of Copyright</b> .....	<b>4</b>
<b>4.0 Introduction</b> .....	<b>5</b>
<b>4.1 The cell's ability to control protein folding:</b> .....	<b>5</b>
<b>4.2 IRE1 signalling:</b> .....	<b>7</b>
<b>4.3 ATF6 signalling:</b> .....	<b>11</b>
<b>4.4 PERK signalling:</b> .....	<b>12</b>
<b>4.5 Activation of the RNase activity by the kinase domain of Ire1:</b> .....	<b>13</b>
<b>4.6 Hac1 processing:</b> .....	<b>14</b>
<b>4.7 BiP recognition of unfolded proteins</b> .....	<b>15</b>
<b>4.8 ERAD induction:</b> .....	<b>16</b>
<b>4.9 Cellular importance of protein kinases:</b> .....	<b>16</b>
<b>4.10 ER stress increases the size of the ER:</b> .....	<b>18</b>
<b>4.11 The role of IRE1 in nutrient sensing:</b> .....	<b>19</b>
<b>4.12 IRE1's ability to control cell fate:</b> .....	<b>20</b>
<b>4.13 The use of phosphomimetics</b> .....	<b>21</b>
<b>4.14 Dcr2 phosphatase:</b> .....	<b>22</b>
<b>4.15 Ptc2 phosphatase:</b> .....	<b>23</b>
<b>4.15 Aims and objectives</b> .....	<b>24</b>
4.15.1 Comparison of $\beta$ -galactosidase reporter assays to determine levels of UPR activation .....	25
4.15.2 Visualisation of Ire1 clustering during ER stress .....	25
<b>5.0 Materials and Methods:</b> .....	<b>26</b>
<b>5.1 Materials</b> .....	<b>26</b>
5.1.1 Buffers and solutions.....	26
5.1.2 Media composition of cell cultures .....	29
5.1.3 Strain information: .....	30
5.1.4 Plasmid information.....	30
<b>5.2 Methods</b> .....	<b>31</b>
5.2.1 Culturing techniques and DTT stress induction: .....	31
5.2.2 E. coli plasmid extraction using Qiagen Plasmid Midi Kit.....	32
5.2.3 Nanodrop quantification of plasmids .....	33
5.2.4 Running agarose gels [137] .....	33
5.2.5 Transformations of yeast cells [138].....	33
5.2.6 Acetate and replica plating:.....	34
5.2.7 Protein extractions for $\beta$ -galactosidase assays .....	35
5.2.8 DC protein assay.....	35
5.2.9 $\beta$ -Galactosidase assay.....	35

5.2.10 Fluorescent confocal microscopy cell culture: .....	36
5.2.11 Microscopy analysis .....	36
5.2.12 Statistical analyses.....	37
<b>6.0 Results: .....</b>	<b>38</b>
<b>6.1 Characterising the effect of phosphatase overexpression on the induction of a UPR-<math>\beta</math>-galactosidase reporter.....</b>	<b>38</b>
6.1.1 Rationale.....	38
6.1.2 Results for the $\beta$ -galactosidase reporter assay.....	39
<b>6.2 Clustering of Ire1 in phosphatase overexpression mutants during ER stress.....</b>	<b>42</b>
6.2.1 Rationale.....	42
6.2.2 Confocal microscopy results.....	43
<b>7.0 Discussion.....</b>	<b>53</b>
7.1 Overexpression of phosphatases on UPR activation during ER stress conditions .....	53
7.2 Foci formation by Ire1 is reduced in DCR2 and PTC2 overexpressing cells .....	54
<b>8.0 Conclusion and future work: .....</b>	<b>56</b>
8.1 Summary of findings.....	56
8.2 Future work.....	57
8.2.1 Identifying phosphorylation state.....	57
8.2.2 Utilising activation-loop mutant strains.....	58
8.2.3 Test cumulative effect of overexpressing both phosphatases.....	58
8.2.4 Investigation into mRNA reduction as the mechanism of action .....	59
<b>9.0 References:.....</b>	<b>59</b>

## 2.0 Acknowledgments

I would like to thank Dr Martin Schroeder for his help and guidance in the practical and writing of my Masters project. In addition to this, I would like to thank fellow Masters student Yesh Tanna and PhD students Hanan Sagini and Amnah Obidan.

Finally, I would like to thank my family for their support during my project and always believing in me.

## 3.0 Statement of Copyright

*“The copyright of this thesis rests with the author. No quotation from it should be published without the author’s prior written consent and information derived from it should be acknowledged.”*

#### 4.0 Introduction:

The correct folding, modification and synthesis of Golgi-bound proteins and proteins designated to be secreted are controlled by the endoplasmic reticulum (ER), a membrane-bound organelle. The purpose of the ER is to correctly fold proteins, therefore, the ER contains a multitude of foldases and molecular chaperones to assist with protein folding [1]. Multiple post-translational modifications also occur in the ER that do not take place in the cytosol, such as glycosylation and disulphide bond formation [1]. The process of modification and folding is sensitive to changes in ER homeostasis and is therefore a highly controlled process. However, perturbations in ER homeostasis such as  $\text{Ca}^{2+}$  depletion, altered glycosylation or hypoxia, can induce ER stress caused by an accumulation of unfolded proteins [1-3]. In response to these ER stressors, the cell has evolved an adaptive pathway to limit the accumulation of unfolded proteins, termed the unfolded protein response (UPR). The UPR attempts to alleviate the build-up of unfolded proteins in a multitude of ways such as downregulating transcription of genes coding for secretory proteins, increasing removal of unfolded proteins via ER-associated degradation (ERAD) [4]. In addition to this the UPR also leads to a rise in the synthesis of ER foldases and chaperones to increase the folding capability of the ER. The size of the ER is also enlarged due to an increase in phospholipid synthesis [5,6]. If activation of the UPR is not sufficient to alleviate the accumulation of unfolded proteins, the cell initiates apoptosis through pathways such as JNK protein kinase and caspases 7, 12 and 3 [7,8].

##### *4.1 The cell's ability to control protein folding:*

For a protein to perform its function it must first fold into a unique three-dimensional arrangement, this fold must then be stable for a biologically relevant time. The folding of a protein is predetermined by its amino acid sequence, this concept is known as Anfinsen's

dogma [9]. This concept was derived from the spontaneous refolding of pure proteins after denaturation, this revealed that all that was necessary for protein folding was the predetermined amino acid sequence [10]. Folding *in vivo* must also involve the use of enzymatic assistance, disulphide exchange, glycosylation enzymes and molecular chaperones all of which reduce the protein folding in non-productive incorrect pathways [10]. The additional folding assistance is required because spontaneous folding follows a route guided by successive drops of free energy, these drops lead to various folded states as the protein folds towards its final arrangement. The different conformations of a protein are only separated by low energy barriers [11]; therefore the folding machinery is important to assist the protein in following the right pathway.

Protein folding *in vivo* occurs in a complex and protein rich solution. It is estimated that the protein concentration of the ER is ~100 mg/ml. At this concentration the possibility of aggregation for proteins inside the ER is high, this is especially true for newly synthesised proteins as they have exposed hydrophobic regions which would not be exposed upon initial folding [10]. Therefore, minimising the risk of aggregation is one of the main roles of molecular chaperones in the ER. ATP is also important in protein folding as many of the chaperones which facilitate; translocation, disulphide bond formation, rescue of misfolded molecules and oligomeric assembly require ATP [10,12].

Cellular proteins are synthesised on ribosomes and the folding that occurs can either be co-translational or post-translational. Co-translational folding occurs before protein synthesis has been completed meaning that the nascent protein has not yet been released from the ribosome [13,14]. Post-translational folding occurs once the whole of the proteins has been synthesised. Much of the folding process is dependent on the environment in which the folding takes place such as in the cytosol or other compartments like the ER [15,16]. Molecular chaperones play a vital role in protein folding. Their role in protein folding can range from interacting with nascent proteins as they are synthesised from the ribosome, to guiding later folding stages [15,16]. To ensure efficient protein folding, multiple molecular chaperones work in tandem on the same protein [13]. Although the molecular chaperones increase the efficiency of the folding process, they themselves do not increase the rate of the steps but rather reduces the number of competing reactions such as aggregation [13]. However, there are some classes of folding catalysts that increase the speed of potentially

slow steps, such as protein disulphide isomerases which increase the rate at which disulphide bonds are formed and reorganise [17]. Molecular chaperones are able to rescue misfolded or even aggregated proteins and give them the ability to fold again correctly, as well as protecting nascent protein [15,16]. For molecular chaperones to operate at full efficiency ATP is required.

Many of the proteins synthesised in a eukaryotic system are destined to be secreted into the extracellular environment. For secretion to take place, proteins are first translocated into the ER where their folding takes place before moving through the Golgi apparatus [13]. The ER contains a broad array of molecular chaperones and folding catalysts but in addition to that the proteins which are folded in the ER must also pass a 'quality-control' check before they can be exported [18,19]. This quality control check involves the use of glycosylation and deglycosylation reactions which allows the proteins which have undergone correct protein folding to be distinguished from proteins which have been misfolded [18].

Disulphide bonds play a vital role in deciding protein folding pathways as they form covalent intermediaries [20] and reduce the number of available protein conformations [10]. Disulphide bonds can form as soon as the required Cys residue is available, however, some disulphide bonds do not form until later on in the protein folding sequence [10,21]. This is because oxidation and correct folding can occur whether the oxidation process occurs post-translationally or co-translationally. This can be accounted for as ER chaperones have the ability to selectively bind near Cys residues and delay oxidation [10]. These observations demonstrate that the ER can control disulphide bond formation and further that the ER can control protein folding.

#### *4.2 IRE1 signalling:*

In metazoans the UPR pathway is complex consisting of three transmembrane receptors: Inositol requiring kinase 1 (IRE1), activating transcription factor 6 (ATF6) and double stranded RNA-activated protein kinase (PKR)-like endoplasmic reticulum receptor kinase (PERK) [22]. In yeast cells the UPR is less complex and consists of only one transmembrane receptor, IRE1 [23]. The three transmembrane proteins are made of three domains. They all possess a luminal domain, cytosolic domain and a transmembrane domain that traverses the ER membrane connecting the luminal domain and cytosolic domain. The luminal domain consists of an amino-terminal which has an important role in sensing

unfolded or misfolded proteins [24]. The transmembrane domain of Ire1 contains the protein serine/threonine kinase domain which plays a vital role during phosphorylation and more specifically trans phosphorylation [24]. The third domain of Ire1 is the cytosolic C-terminal tail, this region is an endoribonuclease domain. The luminal domain of both IRE1 and PERK show many structural and sequence similarities, the crystal structures of the IRE1 luminal domain in yeast and humans display similar structures to one another and to the crystal structure of the PERK luminal domain from humans and mice [25-27]. This would suggest that the mechanism of action for IRE1 and PERK is similar and that it remains conserved between various metazoans. The cytosolic domain of IRE1 and PERK once again show similar properties with both possessing a kinase domain that undergoes trans-autophosphorylation [28-30].

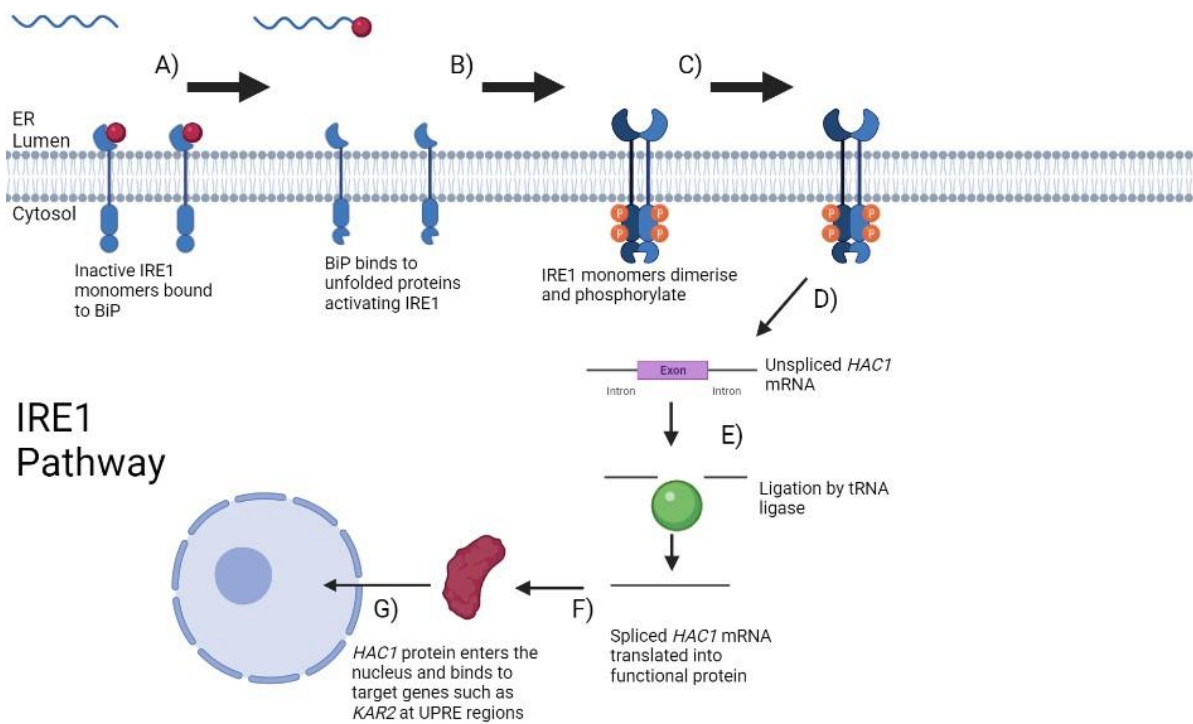
There have been multiple models suggested for the activation of the IRE1 pathway in yeast cells. One model suggests direct binding of unfolded proteins to IRE1, which causes Ire1 to oligomerise. This model has been suggested as the core of Ire1's luminal domain contains two interfaces, interface 1 and interface 2 [25]. Interface 1 creates a deep groove for unfolded proteins to bind to and interface 2 allows oligomerisation, a mutation in either of these interfaces diminishes *HAC1* mRNA splicing [31]. The groove formed by interface 1 in Ire1 are similar to that seen in the major histocompatibility complex (MHC), which can bind peptides with high specificity, which would suggest that Ire1 also binds to unfolded proteins and that the binding potentiates Ire1 oligomerisation [31]. The depth of the groove may also offer the ability to sterically discriminate between folded and unfolded proteins as properly folded proteins would be unable to access the groove [25]. Mutations of residues within the groove have been demonstrated to impair IRE1 signalling in yeast [25,31]. Interaction of IRE1 with peptides also leads to an increase in oligomer species and more recently the human IRE1 luminal domain was shown to bind to both unfolded proteins as well as peptides *in vitro* which displays similarities to the yeast IRE1 luminal domain [31,32]. Karagöz et al., 2017 also suggested through the use of nuclear magnetic resonance that conformation changes occur upon binding of peptides to the groove, the conformational changes are then thought to allow IRE1 oligomerisation and therefore UPR activation.

Another established model is the competition model. This model poses that BiP is bound to the IRE1 luminal domain as a chaperone-substrate type interaction via BiP's substrate binding domain to repress IRE1 [33-36]. The interaction between BiP and IRE1 is

mediated by Erdj4 and occurs at the same site that BiP binds to misfolded proteins. Formation of the BiP, Erdj4 and IRE1 complex stimulates ATPase activity of BiP and causes Erdj4 to dissociate, this leads to monomer formation by IRE1 and inhibition of UPR signalling [34,37]. Nucleotide exchange factor facilitates the exchange between ADP and ATP which leads to dissociation of BiP from the IRE1 luminal domain. During high levels of ER stress, misfolded proteins now compete with the luminal domain of IRE1 for binding to both Erdj4 and BiP, this association of BiP with misfolded proteins impedes BiP binding to IRE1. This inhibition of BiP binding by misfolded proteins enables the IRE1 to dimerise, activating the UPR [34]. In this competition model, the purpose of BiP is to act as a repressor of the UPR by impeding dimerization of IRE1 and not as a direct sensor of ER stress. The core idea of the competition model is the chaperone-substrate type interaction that occurs during binding of IRE1 and BiP [33]. This model is similar to the competitive repression of heat shock factor 1 (Hsf1) activity by Hsp70 [38]. The mechanism by which nucleotide exchange factor allows the exchange of ADP to ATP is similar to the mechanism by which it is achieved in the Hsp70-Hsf1 chaperone system [39]. However, there have been multiple studies that have observed binding between BiP and IRE1 without the need of Erdj4 [40-42].

In addition to the two models proposed above, an additional model called the allosteric model has been suggested. This model differs from the chaperone-substrate type interaction previously suggested as this model indicates an interaction between the luminal domain of Ire1 and the BiP nucleotide binding domain [34,40,41,43]. Another aspect of this model that differentiates itself from the previous models is that misfolded proteins bind exclusively to the substrate binding domain of BiP, which leads to the dissociation of BiP from Ire1 due to conformational change [40,41]. BiP acts as a direct sensor of ER stress in this model as the luminal domain of IRE1 and misfolded proteins bind to different domains of BiP meaning there is no competition for binding sites in this model [40,41]. However, it has been suggested that due to the absence of ATP in this model that it is no longer analogous to the principles used by the nucleotide dependent Hsp70 system [33]. But this model is not a chaperone-substrate type interaction and is therefore more analogous to the mitochondrial Hsp70 during translocation of polypeptides into the inner mitochondrial matrix [44]. Mitochondrial Hsp70 binds to Tim44 primarily through its nucleotide binding domain and not its substrate binding domains which is still available to bind misfolded proteins [45]. Addition of ATP and ADP to

this complex *in vitro* was unable to cause dissociation of mitochondrial Hsp70 from Tim44 suggesting that this interaction is also independent of nucleotides [46]. Therefore, the interaction of BiP and the luminal domain of IRE1 in this model is not so dissimilar from the mechanism used by Hsp70 when it is not in a chaperone-substrate type interaction. Although nucleotides in this model appear to serve a secondary purpose, ATP may sensitise BiP, when bound to IRE1, to engage with misfolded proteins. This is because although in the mitochondrial Hsp70-Tim44 complex ATP and ADP were under able to causes dissociation, when lysates were used dissociation of the complex was increased in the presence of ATP suggesting a role for nucleotides in misfolded protein binding [45,46].



Created in BioRender.com

Figure 1. Allosteric model of the IRE1 pathway of the unfolded protein response. A) Under normal ER conditions BiP (red circle) is bound to inactive Ire1 monomers (blue transmembrane proteins). B) When ER stress occurs and unfolded proteins accumulate, BiP dissociates from Ire1 and binds to the unfolded proteins (blue wavy line). C) Ire1 monomers oligomerise and undergo *trans*- autophosphorylation, activating the endoribonuclease domain (Phosphorylation shown with orange circles on the cytosolic side of the membrane). D) The active endoribonuclease cleaves the *HAC1* mRNA. E) tRNA ligase (Green circle) then ligates the spliced mRNA. F) The newly spliced *HAC1* mRNA is then translated to the functional transcription factor Hac1 (Dark red). G) Hac1 enters the nucleus and binds the UPRE promoter region.

In all the proposed models the signal is propagated by the dimerization or oligomerisation of Ire1, it may be that the luminal domain of Ire1 can be activated in multiple ways and that multiple theories are correct [47]. When ER stress is induced Ire1 forms foci sites which upon ER stress removal are not visible. This clustering of Ire1 was observed in both kinase inactive mutants and *HAC1* knockout mutants [48]. This suggests that clustering of Ire1 is not reliant on kinase activity or UPR gene expression, but that Ire1 clustering is needed for activation of the UPR. Therefore, if Ire1 does not cluster when ER stress is induced then there should be reduced activation of the UPR [25]. This oligomerisation promotes *trans*-autophosphorylation of Ire1 in its activation segment at serine residues 837, 840, 841, 850 and threonine residue 844 [28,49,50], phosphorylation of these residues correlates with activation of Rnase activity [51]. In addition to this, Ire1 mutants that lack the ability to bind BiP have been shown to spontaneously dimerise and activate Rnase activity when there is no or little ER stress, suggesting that Kar2/BiP maintains Ire1 in an inactive state [51]. Once Ire1 has been activated the target of its endoribonuclease domains is the mRNA which encodes the transcription factor Hac1 [52,53]. Activated Ire1 splices the *HAC1* mRNA and excises a 252-nucleotide long intron, the exons are then ligated together by tRNA ligase to create a spliced form of *HAC1*, termed *HAC1<sup>i</sup>* (Figure 1)[54-56]. This type of splicing is unique as most pre-mRNAs require the spliceosome, however, *HAC1* splicing more closely resembles pre-tRNA splicing as only two components are required for cleavage and ligations [57]. The newly created *HAC1<sup>i</sup>* is then translated and enters the nucleus where it binds to a promoter region termed the unfolded protein response element (UPRE) (Figure 1).

#### 4.3 ATF6 signalling:

ATF6 is a type II transmembrane protein, upon unfolded protein accumulation it is packaged into vesicles and transported from the ER and delivered to the Golgi apparatus [58]. Upon reaching the Golgi apparatus, ATF6 interacts with two proteases, S1P and S2P (site-1 and site-2 protease, respectively). S1P removes the luminal domain of ATF6 and S2P removes the transmembrane anchor [59,60]. This cleavage releases the N-terminal cytosolic domain which enters the nucleus of the cell to effect gene expression. This process of releasing the cytosolic domain is known as Regulated Intermembrane Proteolysis (RIP) [61]. This mechanism of activation is similar to and best represented by the sterol regulatory element binding proteins (SREBPs) model, these are transcription factors involved in the synthesis of

cholesterol [62]. These proteins are also found to be embedded in the ER membrane with their NH<sub>2</sub> and COOH-terminals facing into the cytosol, which is similar to ATF6 as its NH<sub>2</sub> terminal also projects into the cytosol (). The process for SREBPs is to bind with SREBP cleavage activating protein (SCAP) which then transports the SREBPs to the Golgi where RIP can occur [63,64]. The membrane-anchored serine protease S1P is then able to cleave the SREBP at a recognition sequence defined as RXXL, where X can be any amino acid [60,65]. This recognition sequence has also been detected in the ATF6 luminal domain suggesting that the model for ATF6 cleavage by S1P and S2P may be similar to that of the SREBP model. However, there has not been an identified molecule which replicates the function of SCAP in the SREBP model, therefore, how ATF6 is transported to the Golgi apparatus remains unclear.

#### 4.4 PERK signalling:

The luminal domain of PERK demonstrates a small amount of homology to the luminal domain of IRE1, their homology is similar enough that the luminal domain of IRE1 can be replaced with that of PERK and still function in yeast even though yeast does not have the PERK pathway [22,66]. The homology of the luminal domains is not the only similarity between PERK and IRE1. PERK and IRE1 are alike since in mammalian cells they both rely on the molecular chaperone BiP, which is bound to both luminal domains, to be released for activation, which for PERK is oligomerisation and *trans*-autophosphorylation [22]. However, it is thought that the way in which BiP suppresses activation of both proteins may differ, as the binding sequence for BiP in IRE1 activation overlaps the regions responsible for oligomerisation and signalling [67]. Whereas the binding sequence of BiP does not overlap the oligomerisation sequence and is therefore believed to prevent activation sterically [66,67]. Once PERK has been activated it phosphorylates eukaryotic initiation factor 2 (eIF2 $\alpha$ ) on serine 51 which rapidly inhibits the initiation of translation [66,68]. Translational initiation requires the formation of the ternary complex which consists of initiator methionine transfer RNA, GTP and eIF2, this complex loads the ribosome with mRNA that's ready to be translated. The ternary complex once bound to the ribosome to form the 43 S preinitiation complex [22]. The preinitiation complex then binds to the 5' cap structure of mRNAs and then in a 5' to 3' way scans the mRNA until it comes to the first AUG codon which allows the 60 S subunit to bind and initiate translation [22]. The combination of the two ribosomal subunits leads the GTP in the preinitiation complex to become hydrolysed to GDP. When eIF2 $\alpha$  becomes

phosphorylated by PERK signalling it binds tightly to eIF2B preventing eIF2B from reducing eIF2 $\psi$ -GDP to eIF2 $\psi$ -GTP which then reduces translation of upstream ORFs which would have been translated when GTP is readily available [69]. After translation has terminated the ribosome dissociates into 60 S and 40 S subunits although the 40 S subunit may remain bound to the mRNA and once a new pre-initiation complex is bound can continue to scan for additional start sites for translation to reinitiate. When low levels of phosphorylated eIF2 $\alpha$  are present upstream ORFs are efficiently translated and downstream ORFs become repressed [22]. Increased amounts of phosphorylated eIF2 $\alpha$  interferes with the GDP-GTP exchange and leads to translation of downstream ORFs which under normal homeostatic conditions would not be translated due to the ribosomes still remaining bound to the mRNA and the pre-initiation complex allowing the ribosome to continue to scan further along the mRNAs before re-initiation [22,69,70]. This mechanism reduces translation of most mRNAs but has been found to actually increase *GCN4* in yeast and *ATF4* in vertebrates [70,71]. ATF4 has been observed to induce expression of ATF3 and CHOP under ER stress, CHOP is vital in the apoptosis pathway and ATF3 has been suggested to bind to the promoter region of *GADD34* [72].

#### 4.5 Activation of the RNase activity by the kinase domain of Ire1:

The N-terminal lobe of protein kinases contains an activation segment which is termed as the region between and including two amino acid motifs, DFG and APE [73]. The Ire1 kinase domain activation segment contains the activation loop, the magnesium binding loop, the  $\beta$ 10 domain and the P+1 region. The activation segment is vital to regulating the RNase activity of Ire1. The activation segment is important because it contains conserved residues thought to be involved in phosphorylation, Ser840, Ser841, Thr844 and Ser850 [50]. The activation loop is believed to promote *trans*-autophosphorylation within the kinase domain at residues, S840 and S841 [28]. An active conformation of the cytosolic domain is believed to be achieved during *trans*-autophosphorylation by neighbouring Ire1 molecules which is then thought to lead to activation of the Ire1 RNase domain [5,74]. Autophosphorylation of S841 and T844 was discovered to be required for activation of the Ire1 kinase domain [50,75,76]. Mass spectroscopy was also able to reveal that as well as S841 and T844 the previously identified sites S840 and S850 were also phosphorylated [28,50]. However, further investigations into S850 found that mutations of the residue did not result in an impaired Ire1 [49]. Another

conserved residue of importance in the activation segment is D828. D828 is a critical residue in the kinase domain of Ire1 as cells possessing mutations in D828 have been described as “kinase dead” [77]. D828 is found in the magnesium binding loop of the activation segment and coordinates the  $\beta$  and  $\gamma$  phosphates of ATP with  $Mg^{2+}$  [78,79]. In addition to this, D797 and K799 residues also have the predicted function of coordinating the  $\gamma$  phosphate of ATP bound to the kinase domain [80]. It has been shown that the use of kinase inhibitors still results in RNase activity [77], suggesting that the activity of the kinase domain may not be required for RNase activation. The activation of the RNase domain may be due to the occupation of adenine and ribose subsites, which are believed to stabilise the kinase active sites in an open conformation which would favour Ire1 self-association [75]. The key to activation of the RNase domain is a conformation change of the kinase domain, resulting from either activation loop interactions [50,73] or by Ire1 self-association [75]. Activation of RNase is what facilitates the splicing of *HAC1* mRNA and induces UPR gene and therefore its activation is important.

#### 4.6 *Hac1* processing:

Hac1p is a basic leucine zipper (bZIP) transcription factor [52] that alters the UPR in yeast. Hac1p is only detectable in cells which are undergoing ER stress and have an activated UPR. Whilst in both stressed and non-stressed cells, Hac1 is detectable in its mRNA forms [54]. Upon UPR activation, spliced *HAC1* mRNA, termed *HAC1<sup>u</sup>*, occurs through a spliceosome independent mechanism and the exons are then ligated together to give *HAC1<sup>i</sup>* [81]. Spliced *HAC1* generated from ER stress is efficiently translated to Hac1p [82-84]. Hac1p is a transcription factor and it therefore contains a nucleus localisation sequence which then directs the protein to enter the nucleus where it can effect gene expression [85] It was also thought that *HAC1<sup>u</sup>* associates with polysomes but stalls on ribosomes when the UPR is not activated [24], however, different ideas about how *HAC1<sup>u</sup>* is controlled have recently arisen [85]. If *HAC1<sup>u</sup>* was translated, a UGA sequence in the intron would cause translation to stop early and result in a shorter protein missing the activation domain which is encoded in the second exon and this is evident using  $\beta$ -galactosidase assays where Hac1<sup>u</sup>p induces weaker activity on the UPRE compared with Hac1<sup>i</sup>p [85,86]. The higher activity of Hac1<sup>i</sup>p is thought to be due to not only the removal of the intron, but also due to the replacement of the last 10 amino acids of Hac1<sup>u</sup>p with 18 amino acids from the second exon [86]. These 18 amino acids act as a transcriptional activation domain, giving Hac1<sup>i</sup>p higher activity [85]. Both Hac1<sup>u</sup>p and

Hac1<sup>p</sup> proteins are degraded with a half-life of around 2 min [56,87,88]. This short half-life indicates that the *HAC1<sup>i</sup>* protein needs to be continuously expressed to allow for continued activation of the UPR. To maintain continuous expression the *HAC1* gene is autoregulated and has its own UPRE region in its promoter allowing for a positive feedback loop upon UPR activation [89]. This loop is only broken when Ire1 and the UPR are inactivated. There have been three promoter elements so far that have been identified to be regulated by the *HAC1* protein. The first, is the unfolded protein response element (UPRE) [90] and it is the main promoter target of the *HAC1* protein as it is the promoter of ER chaperone gene and the majority of UPR target genes. Mammalian cells have the ER-stress response element (ERSE) which is regulated by XBP1 and ATF6 [91]. Other genes not under control of the UPRE promoter but still regulated by the *HAC1* protein have the subtletelomeric ATF/CREB GTA variant element (SACE) [92] or the upstream repressing sequence 1 (URS1) which is mainly found as the promoter for genes involved in nitrogen and carbon utilisation [93].

#### *4.7 BiP recognition of unfolded proteins:*

The role of BiP in the cell is to bind transiently to newly synthesised proteins which are located in the ER. The binding of BiP to misfolded or unassembled proteins assists the folding process of the polypeptides. BiP consists of two major domains, an ATPase N-terminal and a substrate-binding C-terminal [22,94]. Short hydrophobic strands are preferentially bound by BiP, hydrophobic strands can form  $\beta$ -strands which are found deep in the core of folded proteins demonstrating that these exposed hydrophobic strands are part of an unfolded protein [22,94]. Substrates bind to BiP which stimulate its ATPase domain to generate the ADP- bound form of BiP which has high affinity for bound peptides, exchange of ADP with ATP causes the substrate to be released to continue on its folding pathway[22,94]. The ATPase domain is then activated to hydrolyse ATP and return BiP to its high affinity ADP-bound state [22,94]. BiP as well as other HSP70s can cycle between monomeric and oligomeric states. When in its oligomeric state, BiP is post translationally modified by phosphorylation and ADP ribosylation [94-96]. Conditions which increase the number of unfolded proteins in the ER lead to a decrease in BiP modification and an increase in the proportion of monomeric BiP species [22,94,97]. Only monomeric, unmodified forms of BiP associate with unfolded proteins and it has been suggested that oligomeric BiP acts as a storage pool from which additional monomeric BiP forms can be recruited when the levels of unfolded peptides increases [22,94].

#### 4.8 ERAD induction:

Genes involved in ER-associated degradation (ERAD) were identified to be second class targets of the UPR in yeast [6]. ERAD is the mechanism by which proteins that are misfolded or are slowly folding are removed from the ER and degraded [6]. The removal and degradation of accumulating unfolded, or misfolded proteins helps to alleviate the ER stress. The UPR and ERAD are functionally connected to each other. This connection is evident in cells with compromised ERAD as constant UPR activation is observed in these cells as the misfolded proteins are not being removed [98-100]. In mammalian cells, induction of an ER membrane protein, HERP/Mif1, by ATF4 and ATF6 has been suggested to interact with the 26 S proteasome and bring proteosomes into closer proximity to the ER allowing for more efficient degradation [99]. In addition to this, *herp*<sup>-/-</sup> cells display increased UPR signalling suggesting a greater susceptibility to ER stress [101]. Multiple genes involved ERAD require induction by HAC1/XBP1 of the IRE1 pathway such as HRD1, UGGT and EDEM. EDEM is responsible for recognising and targeting the unfolded or misfolded proteins for degradation [102]. It has also been suggested that in mammalian cells the UPR may work in two phases facilitated by the different pathways in the UPR. During phase one, the unfolded proteins are given time to refold without being degraded and phase two degrades any unfolded or misfolded proteins which have been unable to properly fold during phase one [103]. This two-phase mechanism is believed to occur due to ATF6 which activates quicker than IRE1 as IRE1 has to induce the splicing of *HAC1/XBP1* and then wait for translation to an active protein. During the time it takes for *HAC1/XBP1* induction it is thought that the ER chaperones induced by ATF6 are given time to promote protein refolding before activated *HAC1/XBP1* is able to induce genes involved in ERAD [103,104].

#### 4.9 Cellular importance of protein kinases:

Protein kinases are involved in a myriad of cellular process are their role is pivotal in coordinating and regulating gene expression, metabolism, cell division, cell differentiation and cell growth [105]. Protein kinases are one of the largest gene families in eukaryotes [106] which evidences their importance and involvement in a multitude of pathways. Protein kinases share conservation of the overall fold, however, differences in flanking regions and the core sequence of a kinase allows each one to respond to unique signals that control their activity and switch between active and inactive [105]. A region of protein kinases that has been

a major focus is the activation segment as this is the region where phosphorylation is able to control kinase activity [105]. PKA was the first protein kinase structure to be solved, it was in an active phosphorylated state and it was observed that a phosphor-residue located in the activation segment interacted with a positively charged pocket on the protein kinases surface [107]. Early inactive protein kinase structures were unphosphorylated in the activation segment and were able to adopt multiple folding conformations that were distinct from that seen in the active PKA protein kinase [108,109]. It was then later discovered that all protein kinases regulated by phosphorylation in the activation segment have a conserved arginine immediately before a conserved catalytic aspartate in the catalytic loop [105]. These protein kinases were grouped and termed RD kinases. The activation segment encompasses an  $Mg^{2+}$  binding loop, a short  $\beta$  strand, activation loop and  $P + 1$  loop [73]. The activation segment of both tyrosine and serine/threonine protein kinases share structural consistency at they N and C terminal ends whereas the activation loop is was observed to have much greater structural diversity [73]. Therefore, the N and C terminals of the activation segment are known as anchor points. The N-terminal anchor consists of the magnesium binding loop and  $\beta 9$  at the start of the activation segment. The C-terminal anchor consists of the middle of the  $P + 1$  loop and ends at  $\alpha EF$ , a short helix [73]. The most common method for regulating protein kinase activity is through phosphorylation of the activation loop. Upon phosphorylation of at least one residue in the activation loop, the loop refolds and is pinned at the anchor points allowing the phosphorylation loop to be positioned for substrate binding [73]. The electrostatic interaction between the primary phosphate and a basic pocket is vital for this conformation change to occur. As stated previously, arginine is one of the residues that make up the basic pocket and is positioned immediately after the invariant aspartate [105]. Studies utilising mutations of the RD arginine have given evidence for its importance in tyrosine protein kinases as well as serine/threonine protein kinases that require phosphorylation in the activation loop [110,111]. The RD arginine residue due to its position in the catalytic loop is directly connect to the catalytic machinery, however, comparison between the inactive and active structures revealed that the interaction between the RD arginine and the primary phosphate had little effect on catalytic loop position [73]. This suggests that the RD arginine controls the folding of the activation loop which therefore affects the N and C terminal anchor conformation instead of directly relaying the signal to the catalytic loop [73]. Some protein kinases have also been known to have additional phosphorylation sites that do not interact with the RD pocket

known as secondary phosphorylation sites [73]. These additional secondary sites can occur both downstream and upstream of the original primary phosphorylation site.

Primary site phosphorylation is known to be the most common mechanism for protein kinases to position their activation segments there are other ways in which their active conformations can be stabilised. Other options for stabilising the conformations of protein kinases are using separate regulatory proteins, changes in the amino acid sequence within the kinase domain and extensions or insertions to the kinase domain [73]. These methods are sometimes used in conjunction with phosphorylation but in other protein kinases these methods prove sufficient to promote activity without the need for phosphorylation [73].

The importance of the phosphorylation in the activation loop has been previously investigated [49] by inactivating phosphorylation sites by mutating a serine and threonine residues to an alanine residues to mimic unphosphorylated sites. The previous study created IRE1 mutants, S840A S841A T844A S850A (termed Q-A), and S837A S840A S841A T844A S850A (termed P-A) [49]. It was noted that once all phosphorylation sites were inactivated there was still *HAC1* splicing occurring, which may suggest that phosphorylation is not the sole factor in Ire1 activation [49]. However, *HAC1* splicing was observed at an increased level when the phosphorylation sites were unimpeded. The residues S840 and S841 have been suggested to be the most important sites to activate Ire1 suggesting a hierarchy of importance among the phosphorylation sites in the activation loop [49]. Therefore, by utilising these phosphorylation point mutants alongside suggested phosphatases, the targets of the phosphatases may be identified.

#### *4.10 ER stress increases the size of the ER:*

A correlation between ER expansion and ER stress exists. Cell types with high secretory capacity such as hepatocytes or pancreatic exocrine cells have been observed that have an increase in ER size during ER stress (3). This observation can also be made when overexpression wild-type or mutant membrane proteins (141). To investigate the role of the UPR in controlling ER membrane proliferation, UPR deficient strains were created and in yeast this means the cells are inositol auxotroph's [112]. ER stress induced transcription of a key enzyme involved in phospholipid biosynthesis, inositol-1-phosphate synthase (*INO1*). This

induction of *INO1* transcription occurs in an *IRE1* and *HAC1* dependent manner [6,112]. Inositol starvation was reported to activate transcription of *INO1* also in an *IRE1* and *HAC1* dependent manner [112]. From these data it was believed that the UPR was able to control proliferation of the ER membrane through *INO1* regulation. However, further work on the role of the UPR in ER membrane synthesis suggests that the role of the UPR is much more complex. Expression of an inner mitochondrial membrane protein, Acr1P, and an ER membrane proliferation inducing peroxisomal membrane protein, Pex15p, were lethal in *IRE1* deficient yeast cells [113]. The lethality of both Acr1p and Pex15p were rescued by growing the cells on oleate instead of galactose [113]. These observations suggests that the UPR may not have a role in regulating the proliferation of the ER membrane and it may be due to a general phospholipid metabolism defect. Further work using cells which overproduce inositol due to elevated phosphatidic acid levels were used to demonstrate that the UPR is not involved with in activating *INO1* [114]. Defects previously observed in UPR deficient strains during inositol starvation were suppressed in cells with elevated phosphatidic acid levels [114]. This work demonstrated that the UPR is not directly in control of *INO1* expression. The more likely reason for lethality during inositol starvation in cells lacking *IRE1* and *HAC1* is small defects in the ER membrane which is where phospholipid synthesis takes [114]. The small changes in the ER membrane therefore perturb phospholipid precursor pools such as decrease in the availability of phosphatidic acid, which may have led to the transcription of *INO1* being altered in the *ire1Δ* and *hac1Δ* cells. Further support for this conclusion is the finding that the *INO1* transcription repressor, Opi1p, is held to the ER membrane through binding with phosphatidic acid in the ER membrane and is complexed there with Scs2p keeping it in an inactive state [115]. If cellular inositol levels increase, then phosphatidic acid is converted into phosphatidylinositol which releases Opi1p from the ER membrane and leads to repression of *INO1*.

#### 4.11 The role of *IRE1* in nutrient sensing:

ER stress has been observed in cells considered to be healthy or unstressed. Splicing of *HAC1* mRNA has been observed in exponentially growing yeast cells, with splicing of *HAC1* between 3% and 30% [83,116]. This provides evidence that even in healthy cells there is a low-level activation of the UPR. This low-level of activation may demonstrate the function of the

UPR to alter the folding capacity of the ER, even when no external ER stressor is added. In addition to this, the level of UPR activation is closely connected to the metabolic condition of the cell. Activation of the UPR is low on easily fermentable carbon sources such as glucose, is moderately increased on less easily fermentable sources such as disaccharides and much higher on nonfermentable carbon sources such as ethanol or acetate [83,116]. The level of *HAC1* splicing is also dependent on the availability of nitrogen sources, nitrogen starvation inhibits splicing and addition of ammonium salts is able to reactivate splicing [116]. In diploid yeast cells, pseudohyphal growth is induced upon nitrogen starvation, this also occurs in cells with defects in the UPR [116]. When the UPR is induced by ER stressors such as tunicamycin pseudohyphal growth is inhibited, the same observation was made in cells overexpressing the *HAC1* protein demonstrating that the UPR has a role in repressing pseudohyphal growth in response to nitrogen [116]. On the basis of these observations, a role in nutrient sensing for the UPR has been proposed.

#### *4.12 IRE1's ability to control cell fate:*

The UPR has the ability to initiate proapoptotic pathways as well as inducing genes that assist the recovery of the ER during ER stress. The ER apoptotic pathways are split into two major groups, the intrinsic pathway and the extrinsic pathway. The intrinsic pathway is responsible for intracellular problems such as DNA damage. The extrinsic pathway focuses on extracellular stimulus. The intrinsic pathway activates upon insertion of oligomeric Bak and Bax into the membrane of the ER, this causes an efflux of calcium ions from the ER [117,118]. The efflux of calcium ions causes the cytosolic level of calcium ions to increase which activate calpain [119]. The activated calpain then cleaves ER-localised procaspase-12 and activates it [119]. The now activated caspase-12 cleaves procaspase-9 which activates it, caspase-9 then activates the executioner caspase which is procaspase-3 [120]. The calcium ions released from the ER are taken up by the mitochondria, leading to a collapse of the inner membrane potential. The uptake of additional calcium ions leads to the permeability transition pore (PTP) being opened [121]. Cytochrome *c* is then released into the cytoplasm through the now open PTP where the apoptosome is formed and procaspase-3 is also activated. The extrinsic pathway is activated when a trimeric complex is formed between IRE1, tumour necrosis factor receptor-associated factor 2 (TRAF2) and apoptosis signal-regulating kinase 1 (ASK1). The

formation of this trimeric complex activates ASK1 and c-Jun amino-terminal kinase and eventually leads to cell death [122]. It is thought that TRAF2 promotes procaspase-12 clustering and when ER stress occurs TRAF2 is released from procaspase-12, most likely through sequestering IRE1 [123].

#### 4.13 The use of phosphomimetics:

In addition to the use of mutations which prevent phosphorylation at specific residues, studies have made use of phosphomimetic mutations which mimic phosphorylated residues [79]. The mutated strains contained an Ire1 protein with mutations S840D-S841D-T844D, which changes serine to aspartic acid. The mutations which were used to mimic consistent phosphorylation did cause Ire1 to be activated and no *HAC1* splicing was observed, however, once an ER stressor was added, activation of Ire1 occurred [79]. This may suggest an alternative activation mechanism is involved or it may also support the chaperone inhibition model of Ire1, as BiP would still be bound to Ire1 until unfolded proteins were present. It was also observed that once the ER stressor had been washed out *HAC1* splicing was observed for a longer period of time than wild type cells [79]. This could suggest that because the phosphomimetic mutants cannot be dephosphorylated that this caused Ire1 to remain active for a longer period time or that the mutations had dysregulated the wild type Ire1 pathway and the cell utilised a less efficient method to cope with the ER stress.

Phosphomimetic mutations may not be an accurate substitution for the residues they are replacing. This may be evident in Chawla *et al.*, 2011 where there was no positive effect of the mutations but instead a negative effect of persistent *HAC1* splicing was observed. The use of phosphomimetics may appear to be appealing as aspartic acid residues appear similar to phosphoserine as they both contain a carboxylate group; however, it has many differences which make its use problematic. Firstly, the carboxylate of aspartic acid only contains one negative charge whereas phosphoserine has two negative charges in its phosphate group. In addition to this, the aspartic acid residue is smaller than phosphoserine, both of these differences suggest that aspartic acid may not be able to actually represent a phosphorylated serine residue [124]. This may be the reason that the abnormal *HAC1* splicing was seen in Chawla *et al.*, 2011 as the mutants could not represent wild type morphology. Another reason for this *HAC1* splicing activity may be the type of ER stressor used. Tunicamycin is a well-known ER stressor as it is able to interfere with glycosylation which allows it to activate the

UPR. However, tunicamycin has the ability to incorporate itself into cell membrane due to its long chain fatty acyl group which may prevent the ER stressor from being removed during washing steps. The problem of removing tunicamycin has been noted in previous studies [125,126] suggesting that if tunicamycin cannot be removed then inhibition of glycosylation will continue, however these studies do not use intact yeast cells. The difficulty of removing tunicamycin may suggest that an alternative ER stressor may need to be used instead, such as dithiothreitol (DTT) which does not incorporate itself into cell membranes and is therefore may be easier to wash out. A comparison on growth of cells after treatment with either tunicamycin or DTT was conducted and showed that tunicamycin treated cells were not able to reach the growth level of wild type cells when tunicamycin was washed, whereas cells treated with DTT demonstrated a dose-dependent manner of growth, with longer periods of exposure having a greater impact on growth after treatment with DTT [127].

#### 4.14 *Dcr2* phosphatase:

Dose-dependent cell cycle regulator 2 (*Dcr2*) is a phosphatase which has been previously suggested to dephosphorylate *Ire1*, originally studied due to observed pro-mitogenic effects [128]. To investigate *Dcr2*'s interaction with *Ire1*, two mutant strains were used, one replaced serine with glutamic acid to represent phosphorylated residues (*IRE1-S840E-S841E*) and the other replaced serine with alanine to represent unphosphorylated residues (*IRE1-S840A-S8941A*) [128]. By using cobalt ion beads it was found that the *Dcr2* phosphatase co-precipitated with the *IRE1-S840E-S841E* mutant but not with the wild type or alanine mutants [128]. These results suggest that *Dcr2* physically interacts with the phosphorylated form, which in this study is a glutamic acid residue, meaning *Dcr2* may play a role in *Ire1* dephosphorylation. However, *ire1Δ dcr2Δ* double mutants did not proliferate at the same rate as *ire1Δ* or *dcr2Δ* single mutant strains, suggesting that *Dcr2* does not act only on *Ire1* but may have a general effect on cell proliferation [128]. This may be in line with a previous study implicating *Dcr2* in cell cycle progression [129]. In *S. cerevisiae* a point known as START is of interest in cell cycle progression as when cells pass through this START point they are committed to cell division [129]. Loss of *DCR2* caused a delay in cells reaching START and overexpression altered cell cycle progression [129], however *DCR2* mRNA levels are not regulated by the cell cycle [130]. When histidine 338 is mutated to alanine a mutant which maintains activity in its substrate binding domain but has its catalytic ability impaired is

generated [131,132]. During the investigation of *DCR2* and its roles in the cell cycle, cells which overexpressed *DCR2* as well as the *DCR2-H338A* mutant were observed to lack an increase in budding which had previously been seen in cells only overexpressing *DCR2* [130], this demonstrates the *DCR2-H338A* mutants ability to antagonise *DCR2*. Previous work by Armstrong *et al* 2017, investigated the effect of Dcr2 overexpression through the use of a 2  $\mu$  plasmid and *GAL1* promoter. Armstrong *et al* 2017, found that overexpression of WT Dcr2 and H388A-Dcr2 inhibited growth of unstressed cells but didn't affect cell survival during cell stress. Deletion of *Ire1* was able to mask the effects of WT Dcr2 and H388A-Dcr2 on unstressed cell growth but did not affect *ire1/1* cell survival during ER stress[49], this suggests that Dcr2 overexpression does not affect survival of ER stress [49].

#### 4.15 *Ptc2* phosphatase:

*Ptc2* is a serine/threonine phosphatase of type 2C and has also been previously suggested to be a negative regulator of *Ire1* in the UPR. In this study, *Ptc2* was shown to be specific to phosphorylated *Ire1* through the use of glutathione-Sepharose beads. Firstly, the *Ire1* proteins were used in its dephosphorylated state and the amount of *Ptc2* obtained was similar to the control, however, when the beads containing *Ire1* protein were incubated in kinase buffer with ATP, the amount of *Ptc2* obtained was 4-fold higher than the control [133]. This would demonstrate that *Ptc2* only binds to *Ire1* when it is in its phosphorylated form and interacts physically with *Ire1*. *Ptc2* was also shown to affect *HAC1* mRNA splicing as overexpression of *Ptc2* decreased *HAC1* splicing by around 50%, whereas deletions of *PTC2* or overexpression of *PTC2* mutants caused *HAC1* to be cleaved even without the addition of an ER stressor [133]. This would suggest that the UPR has become dysregulated in the deletion mutant strains, but overexpression of wild type may confirm that *Ptc2* is a negative regulator and that it acts before *HAC1* splicing. Overexpression of wild-type *Ptc2* was observed to inhibit growth when compared to *Ptc2* mutants. The level of expression was similar as both wild-type and mutant were under control of the same promoter [133]. It was also noted that when tunicamycin was added, the growth of *Ptc2* wild-type overexpression cells was significantly slowed compared to wild-type and mutant overexpression [133]. This indicates that the UPR had been dysregulated during wild-type overexpression. Overexpression of *ptc2* but not E37A-D38A-*PTC2* inhibits cells growth when under ER stress, however, this effect is not seen in cells lacking *Ire1* or P-A-*Ire1* mutants [49]. This data demonstrates that if all potential

phosphorylation sites in the Ire1 activation loop are mutated then the effect of *ptc2* overexpression is nullified. It was also suggested by Armstrong *et al* 2017, that phosphorylation site mutants may have impaired ATP binding and that this leads to a decrease in Ire1 kinase activity and therefore less phosphorylation in other Ire1 regions. This therefore suggests that Ptc2 could dephosphorylate regions other than that of the Ire1 activation loop.

#### 4.15 Aims and objectives

The purpose of this project is to investigate inactivation of the UPR and the components that contribute to IRE1 inactivation. The mechanism of inactivation is still poorly understood but there are phosphatases which have been suggested to be negative regulators of IRE1, these are the protein phosphatases Dcr2 and Ptc2 [128,133]. Re-characterisation of both the Dcr2 and Ptc2 phosphatases is needed as their role in Ire1 is unclear. Armstrong *et al.*, 2017 demonstrated that mutation of all phosphorylation loop sites did not impact on the inactivation of Ire1 suggesting that a different mechanism than dephosphorylation is involved in inactivation. Previous experiments in the Schroeder group have shown that Ptc2 can reduce steady-state levels of mRNAs not regulated by Hac1i, such as *ACT1*, *CYC1* and *PGK1*, this therefore raises the possibility that Ptc2 may act by inhibiting transcription rather than dephosphorylation of Ire1. The purpose of re-investigating Dcr2 comes from the ER stress survival assays performed by Armstrong *et al.*, 2017 which suggested that Dcr2 had no effect on the UPR which disagree with previous work by Guo & Polymenis., 2006.

The aim of this study was to investigate how the phosphatase Ptc2 may regulate Ire1 if previous work has suggested phosphorylation sites do not affect Ire1 inactivation. A re-investigation into Dcr2 would add evidence to whether Dcr2 effects the UPR, which has been previously suggested as a negative regulator of the UPR by Guo & Polymenis., 2016 and also to not have a role in the UPR by Armstrong *et al.*, 2017. The aims were; 1. To investigate how overexpression of Ptc2 and Dcr2 effects expression levels of the UPR-*lacZ* reporter. 2. To observe if Dcr2 or Ptc2 overexpression decreases clustering of Ire1. These goals were achieved using mutant strains of *Saccharomyces cerevisiae*, deletion strains of *DCR2* and *PTC2* individually and combined as well as strains overexpressing either *DCR2* or *PTC2*. By comparing cells either lacking or overexpressing phosphatases to wild type cells the ability of the phosphatases to affect Ire1 and the UPR could be characterised. If the hypothesis that

Dcr2 and Ptc2 are negative regulators of Ire1 and the UPR is true, then a reduction in the activity of the UPR should occur compared with wild type cells. To activate the UPR, 2 mM dithiothreitol will be used to stress the ER of the cells.

#### 4.15.1 Comparison of $\beta$ -galactosidase reporter assays to determine levels of UPR activation

Unstressed cells do not readily splice *HAC1* mRNA, however, when an ER stressor such as DTT is introduced the UPR becomes active and *HAC1* mRNA gets spliced and ligated to produce translatable *Hac1<sup>i</sup>* [81]. Translation of *Hac1<sup>i</sup>* into an active protein leads to expression of UPR-associated genes, which is detected with this reporter assay. By utilising the  $\beta$ -galactosidase reporter assay, quantification of the UPR-associated reporter protein,  $\beta$ -galactosidase, present in the cell lysate will be measured allowing for comparison between the wild-type and mutant strains ER stress signals. Therefore, if the investigated phosphatases are able to significantly decrease expression of the UPR-*lacZ* reporter when compared to wild-type cells, then the phosphatase will be considered a negative regulator and can be used for any additional assays. Conversely, if a phosphatase is not able to sufficiently decrease expression of the UPR-*lacZ* reporter, then the phosphatase will not be taken further when considering additional  $\beta$ -galactosidase assays.

#### 4.15.2 Visualisation of Ire1 clustering during ER stress

Negative regulation of Ire1 has been demonstrated to work without activation loop phosphorylation sites present [49] suggested a different mechanism of negative regulation such as interference with Ire1 clustering. Interference of foci formation has been previously investigated by Armstrong *et al.*, 2017 and suggested that Ptc2 and Dcr2 do not affect clustering. However, this investigation was purely qualitative and further investigation into clustering using quantitative approaches may reveal more. Activation of the Ire1 luminal domain is known to lead to clustering of Ire1 [48]. To observe this clustering *in vivo*, fluorescence microscopy was used. To observe Ire1 clustering in real time, the Ire1 was labelled using mCherry. In addition to this, Sec63 protein was also labelled using GFP to allow visualisation of the cell membranes and therefore observe the location of Ire1 clusters. Using real time *in vivo* imaging allows for confirmation that any decrease seen in UPR activation is not a result of improper Ire1 clustering during ER stress. Therefore, if a phosphatase is able to significantly reduce the clustering of IRE1, which was quantified through fluorescence and

the number of particles per cell, then it may be suggested that the mechanism by which the phosphatases regulate the UPR is through interference of foci formation of Ire1.

## 5.0 Materials and Methods:

### 5.1 Materials

#### 5.1.1 Buffers and solutions:

The composition of general solution used in the work presented in this paper have been described in Table 1.

**Table 1.** General Solutions.

<b>Solution</b>	<b>Quantity</b>	<b>Recipe</b>
<b>EDTA, 0.5 M</b>	500 ml	1. Dissolve 93.1 g Na <sub>2</sub> EDTA·2H <sub>2</sub> O in ~350 ml H <sub>2</sub> O. 2. Adjust pH to 8.0 with 10 M NaOH (~25 ml) 3. Add H <sub>2</sub> O to 500 ml. Autoclave.
<b>MgCl<sub>2</sub>, 1 M</b>	100 ml	1. Dissolve 20.33 g MgCl <sub>2</sub> ·6 H <sub>2</sub> O in ~ 80 ml H <sub>2</sub> O. 2. Add H <sub>2</sub> O to 100 ml. Autoclave.
<b>Na<sub>2</sub>CO<sub>3</sub>, 1 M</b>	500 ml	1. Dissolve 53.0 g Na <sub>2</sub> CO <sub>3</sub> in ~ 400 ml H <sub>2</sub> O. Add H <sub>2</sub> O to 500 ml.
<b>NaH<sub>2</sub>PO<sub>4</sub>, 0.2 M</b>	500 ml	1. Dissolve 12 g NaH <sub>2</sub> PO <sub>4</sub> in ~400 ml H <sub>2</sub> O. 2. Add H <sub>2</sub> O to 500 ml. Autoclave.
<b>Na<sub>2</sub>HPO<sub>4</sub>, 0.2 M</b>	500 ml	1. Dissolve 14.2 g Na <sub>2</sub> HPO <sub>4</sub> (35.82 g Na <sub>2</sub> HPO <sub>4</sub> ·12 H <sub>2</sub> O) in ~400 ml H <sub>2</sub> O. 2. Add H <sub>2</sub> O to 500 ml. Autoclave.
<b>NaOAc (pH 6.0), 3 M</b>	100 ml	1. Dissolve 40.83 g NaOAc·3H <sub>2</sub> O in ~60 ml H <sub>2</sub> O. 2. Adjust pH to 6.0 with glacial HOAc 3. Add H <sub>2</sub> O to 100 ml. Autoclave.
<b>NaOH, 10 M</b>	500 ml	1. Dissolve 200 g NaOH in ~350 ml H <sub>2</sub> O. <i>Solution will get very hot!</i> 2. Store in a polyethylene bottle.
<b>10% (w/v) SDS</b>	500 ml	1. Dissolve 50 g SDS in ~450 ml H <sub>2</sub> O. 2. Add H <sub>2</sub> O to 500 ml. Do NOT autoclave.
<b>Tris·HCl (pH 6.8), 1 M</b>	1 L	1. Dissolve 121.14 g Tris in ~800 ml H <sub>2</sub> O.

		<p>2. Adjust pH to 6.8 with conc. HCl (~ 42 ml).</p> <p>3. Add H<sub>2</sub>O to 1 l.</p> <p>Autoclave.</p>
<b>Tris-HCl (pH 8.0), 1 M</b>	1 L	<p>1. Dissolve 121.14 g Tris in ~800 ml H<sub>2</sub>O.</p> <p>2. Adjust pH to 8.0 with conc. HCl (~ 42 ml).</p> <p>3. Add H<sub>2</sub>O to 1 l.</p> <p>Autoclave.</p>
<b>10% (v/v) Tween 20</b>	50 ml	<p>1. Dissolve 5.55 g Tween 20 in ~ 40 ml autoclaved H<sub>2</sub>O.</p> <p>2. Add H<sub>2</sub>O to 50 ml.</p> <p>Filter sterilize.</p>
<b>50 x TAE</b>	1 L	<p>242 g Tris</p> <p>57.1 ml HOAc</p> <p>37.2 g Na<sub>2</sub>EDTA·2H<sub>2</sub>O</p> <p>Add H<sub>2</sub>O to 1 l</p>
<b>10 x PBS</b>	4 L	<p>320 g NaCl</p> <p>8 g KCl</p> <p>57.6 g Na<sub>2</sub>HPO<sub>4</sub></p> <p>8 g KH<sub>2</sub>PO<sub>4</sub></p> <p>Add H<sub>2</sub>O to 4 l</p> <p>Autoclave</p>
<b>10 x TE (pH 8.0)</b>	4 L	<p>400 ml 1 M Tris-HCl (pH 8.0)</p> <p>80 ml 0.5 M EDTA</p> <p>Add H<sub>2</sub>O to 4 l</p> <p>Autoclave</p>
<b>50 mg/ml ampicillin</b>	50 ml	<p>2.5 g ampicillin, sodium salt</p> <p>Dissolve in ~40 ml H<sub>2</sub>O, add H<sub>2</sub>O to 50 ml, and filter sterilize. Store in 1.0 ml aliquots at -20°C.</p>
<b>2 x assay buffer</b>	400 ml	<p>177 ml 0.4 M Na<sub>2</sub>HPO<sub>4</sub></p> <p>23 ml 0.4 M NaH<sub>2</sub>PO<sub>4</sub></p> <p>0.8 ml 1 M MgCl<sub>2</sub></p> <p>2.8 ml γ-mercaptoethanol</p> <p>532 mg 2-nitrophenyl-β-D-galacto pyranoside</p> <p>Add H<sub>2</sub>O to 400 ml and mix. Store in 50 ml aliquots at -20°C.</p>
<b>1 M dithiothreitol</b>	10 ml	<p>1.54 g dithiothreitol</p> <p>Dissolve in ~ 9 ml H<sub>2</sub>O.</p> <p>Add H<sub>2</sub>O to 10 ml.</p> <p>Filter sterilize.</p> <p>Store at -20°C.</p>
<b>30% (v/v) glycerol</b>	500 ml	<p>189 g glycerol</p> <p>Add H<sub>2</sub>O to ~400 ml, mix well by stirring.</p> <p>Add H<sub>2</sub>O to 500 ml and autoclave.</p>
<b>1 M LiOAc</b>	250 ml	<p>25.50 g LiOAc·2H<sub>2</sub>O</p>

		Dissolve in ~200 ml H <sub>2</sub> O. Add H <sub>2</sub> O to 250 ml. Filter sterilize.
<b>50% (w/v) PEG 4000</b>	500 ml	250 g PEG 4000 Add ~200 ml H <sub>2</sub> O Stir for a few minutes, add H <sub>2</sub> O to ~ 450 ml, stir until PEG4000 is nearly completely dissolved, add H <sub>2</sub> O to 500 ml and mix. Filter sterilise.
<b>Bicinchoninic acid protein assay working solution.</b>	15 ml	Mix 50 parts of reagent A with 1 part of reagent B. Note: when mixing reagents A and B a white precipitate may form [Cu(OH) <sub>2</sub> ] this will dissolve upon further mixing of the reagents.
<b>Reagent A</b>		10 g/l bicinchoninic acid disodium salt, 20 g/l Na <sub>2</sub> CO <sub>3</sub> ·H <sub>2</sub> O 1.6 g/l disodium tartrate, 4.0 g/l NaOH, 9.5 g/l NaHCO <sub>3</sub> . Adjusted to pH 11.25 with 10 M NaOH.
<b>YPac plates</b>	1L	10 g KOAc 20 g yeast extract 20 g peptone 20 g agar

### 5.1.2 Media composition of cell cultures:

Yeast cells were grown in YPD (ForMedium, Norfolk, UK. Cat. No. CCM0202) or in synthetic medium. The synthetic medium was prepared with 2% (w/v) glucose (Fluka #49138), 0.67% (w/v) yeast nitrogen base without amino acids (ForMedium #CYN0405) and 2% agar (ForMedium #AGA03). To make plates, 2% (w/v) agar was added before autoclaving the medium. Concentrations of amino acids were added as outlined below in Table 2. For  $\beta$ -galactosidase assay experiments the deletion strains were grown using uracil dropout media. Overexpression strains were grown on synthetic media using 2% (w/v) galactose (Apollo Scientific, Stockport, Cheshire, UK, #59-23-4), 1% raffinose (Apollo Scientific, Stockport, Cheshire, UK, #17629-30-0)) with uracil and adenine amino acid dropouts. Strains grown for microscopy were also grown on 2% (w/v) galactose, 1% (w/v) raffinose media but with uracil, adenine and leucine amino acid dropouts.

**Table 2.** The amino acid components used and their concentrations for synthetic media broth. For the creation of synthetic media plates, 2% (w/v) agar was added.

Component	Supplier	Cat. No.	Concentration (mg/L)
L-Tyr	ForMedium, Norfolk, UK	DOC0192	30.00
L-Arg-HCl	Sigma-Aldrich, Cramlington, UK	W38 191-8	20.01
L-His-HCl	ForMedium, Norfolk, UK	DOC0144	20.01
L-Met	ForMedium, Norfolk, UK	DOC0168	20.01
L-Trp	ForMedium, Norfolk, UK	DOC0188	20.01
L-Ile	ForMedium, Norfolk, UK	DOC0152	30.02
L-Lys-HCl	ForMedium, Norfolk, UK	DOC0161	30.02
L-Val	ForMedium, Norfolk, UK	DOC197	150.12
L-Ser	ForMedium, Norfolk, UK	DOC0191	375.30
Adenine SO <sub>4</sub>	ForMedium, Norfolk, UK	DOC0229	20.00
L-Phe	ForMedium, Norfolk, UK	DOC0173	50.01
L-Glu	Calbiochem, Watford, UK	3510	100.02
L-Leu	ForMedium, Norfolk, UK	DOC0157	100.20
L-Asp	ForMedium, Norfolk, UK	DOC0121	100.00
L-Thr	ForMedium, Norfolk, UK	DOC0185	199.92

### 5.1.3 Strain information:

In this study different strains of *S. cerevisiae* were used for different experiments. *Escherichia. coli* was also used for bacterial work.

**Table 3.** *E. coli* and *S. cerevisiae* strain information. XL10-GOLD was used for bacterial transformations and plasmid extractions. PWY260 was used for  $\beta$ -galactosidase assays and MSY14-02 was used for microscopy.

Strain Name	Genotype	Organism
<b>XL10-GOLD</b>	<i>Tetr<sup>r</sup> (mcrA)183<sup>r</sup> (mcrCB-hsdSMR-mrr)173 endA1 supE44 thi-1 recA1 gyrA96 relA1 lac Hte [F<sup>r</sup> proAB lacIqZ<sup>r</sup> iM15 Tn10 (Tet<sup>r</sup>) Amy Cam<sup>r</sup></i>	<i>E. coli</i>
<b>PWY260</b>	W303 MATa <i>ire1<sup>Δ</sup>::TRP1 ade2-1 can1-100 his3-11,-15::HIS3<sup>+</sup>UPRE-lacZ leu2-3,-112::LEU2+UPRE-lacZ trp1-1 ura3-1</i>	<i>S. cerevisiae</i>
<b>MSY14-02 [49]</b>	W303 MATa <i>can1-100 ade2-1oc his3-11,-15 leu2-3,-112 trp1-1 ura3-1 Gal+ Suc+<sup>r</sup> ire1::kanMX2</i>	<i>S. cerevisiae</i>
<b>MSY 793-06 [49]</b>	<i>ire1Δ::TRP1 ptc2Δ::kanMX2 his3-11,15::HIS3+ UPRE-lacZ leu2-3,112::LEU2+ UPRE-lacZ</i>	<i>S. cerevisiae</i>
<b>MSY 796-02 [49]</b>	<i>ire1Δ::TRP1 dcr2Δ::kanMX2 ptc2Δ::hphNT1 his3-11,15::HIS3+UPRE-lacZ leu2-3,112::LEU2+ UPRE-lacZ</i>	<i>S. cerevisiae</i>
<b>MSY 792-02 [49]</b>	<i>ire1Δ::TRP1 dcr2Δ::kanMX2 his3-11,15::HIS3+ UPRE-lacZ leu2-3,112::LEU2+ UPRE-lacZ</i>	<i>S. cerevisiae</i>

### 5.1.4 Plasmid information:

Plasmids were first transformed into *E. coli* before being extracted and transformed into yeast. Figure 2 shows the plasmid information for each plasmid such as amino acid markers. Figure 2 A) and C) had the *URA3* (uracil) marker, B) has the *ADE2* (adenine) marker and D) had the *LEU2* (leucine) marker. Plasmids pEvA97 [134] and pJK59 [135] were transformed into MSY14-02, Table 3, and used for microscopy as they contain *IRE1-mCherry* and *Sec63-GFP*, respectively, Figure 6. The pRSII422 [136] plasmid was used for both microscopy and  $\beta$ -galactosidase assays as this plasmid contained the phosphatases being

investigated. Finally, the YCplac33-IRE1-HA (Schroeder lab, Durham University, UK) plasmid was used for  $\beta$ -galactosidase assays.

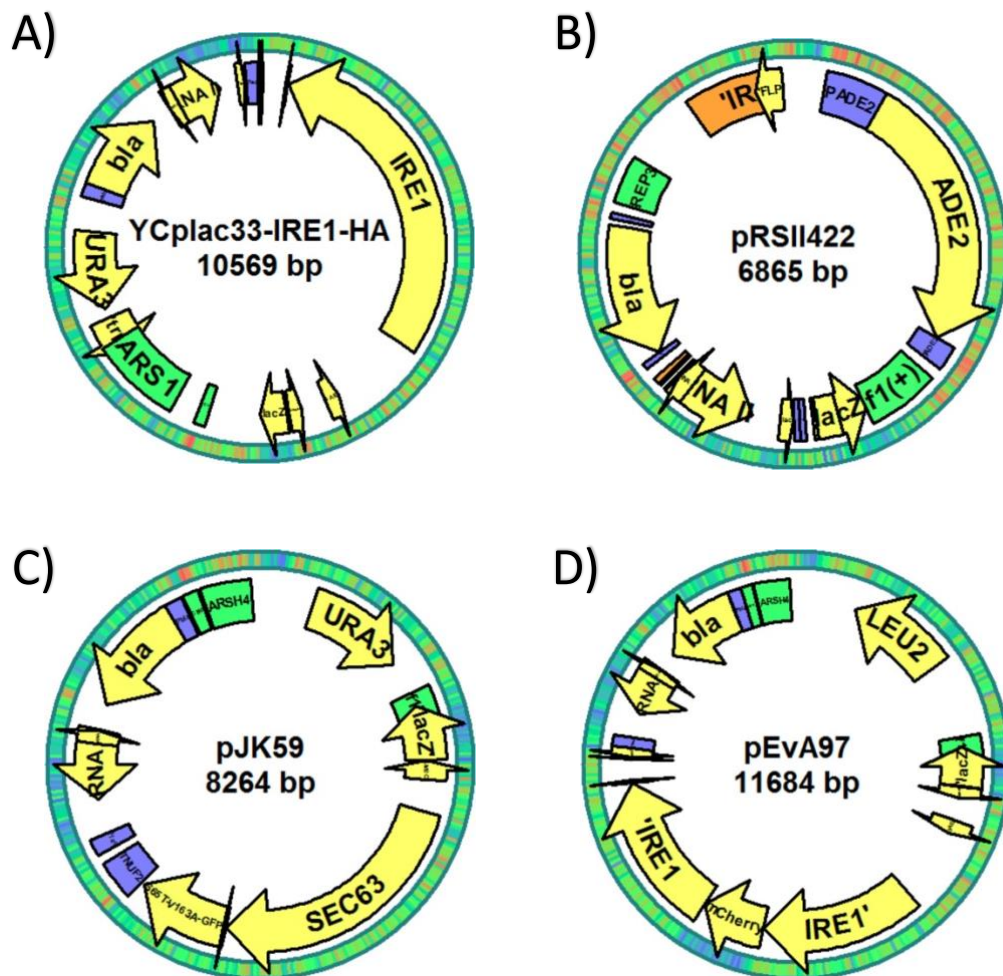


Figure 2. The different plasmids used in transformations of *S. cerevisiae* for microscopy and  $\beta$ -galactosidase assays.

## 5.2 Methods:

### 5.2.1 Culturing techniques and DTT stress induction:

A colony was taken from the plates and cultured in a 4 ml preculture of either YPD or SD media depending on intended use for 24 h at 30 °C at ~220 rpm. The preculture was then used to inoculate a larger culture by using a cell density meter (WPA, Cambridge, UK, model no. CO8000) to take an optical density reading at 600 nm (OD<sub>600</sub>). All experiments using *S. cerevisiae* used the same culture parameters, incubation in a rotary incubator at ~ 220 rpm and a temperature of 30 °C. The stressing of the cells was also achieved the same way in all experiments with the addition 2 mM DTT from a 1 M stock solution.

Sampling was utilised for *β-galactosidase* assays so that consecutive time points of the same culture could be assessed. Strains which contained phosphatase deletions in either a single phosphatase or both were grown in SD media lacking uracil additional strains lacking IRE1 in addition to the phosphatase deletion were also grown in the same media. Strains which overexpressed individual phosphatases were grown in SD media lacking Uracil and Adenine. All strains were initially added to 2ml of SD strain appropriate media which acted as a preculture. The 2 ml preculture was then used to inoculate a larger volume of 155 ml of strain appropriate media which were then left for ~48 h. Once the culture had grown to within the desired OD<sub>600</sub> range, 0.3- 0.6 a 50 ml sample from each culture was taken, spun at 3750 x g for 2 min at 4 °C, the supernatant was then discarded and the remaining pellet was frozen using liquid nitrogen and stored at – 20 °C. The remainder of culture was then treated with 2 mM of DTT from a 1 M stock, further 50 ml samples were then taken at 1 h and 2 h time points, samples were treated as before. Once all time points had been collected and frozen the pellets were thawed and placed onto ice. 1 ml of sterile water then added to each tube and mixed to resuspend the pellet, the cell suspension was then transferred to a 1.5 ml microcentrifuge tube.

#### 5.2.2 *E. coli* plasmid extraction using Qiagen Plasmid Midi Kit:

*E. coli*, XL10-Gold precultures were grown to saturation overnight in LB broth (Formedium, #LBX1L) containing 50 µg ml<sup>-1</sup> of ampicillin at ~230 rpm and 37 °C. These precultures were then added to larger cultures in a 1/100 volume ratio of LB broth and ampicillin and grown until an OD<sub>600</sub> value of 1.5-2.0 was reached. After this the cultures were centrifuged at 4,750 x g for 15 min at 4 °C. The supernatant was then discarded. The Qiagen kit was then used according to manufacturer's instructions.

#### 5.2.3 Nanodrop quantification of plasmids:

Plasmid concentrations were quantified using a NanoDrop (NanoDrop<sup>TM</sup> 1000, Thermo Fisher Scientific, Loughborough, UK) on factory settings.

#### 5.2.4 Running agarose gels [137]:

By dissolving agarose powder in 1 X TAE buffer a 1 % (w/v) agarose gel was cast after being heated using a microwave. To stain the gel 0.5 µg per ml of ethidium bromide was

added, once the agarose had cooled. To prepare the samples for running on the gel 2  $\mu$ l of 6 X loading buffer (Thermo Fisher Scientific, cat. No. #R0611), 9  $\mu$ l of water and 1  $\mu$ l of plasmid obtained by miniprep were mixed before adding to the well. The gel was placed into a tank which was filled with 1 X TAE buffer, Table 1. The samples were loaded into the lanes, with the first lane containing 5  $\mu$ l of Gene Ruler DNA ladder 1 kb (Thermo Fisher Scientific, United States, cat. No. #SM0331).

#### *5.2.5 Transformations of yeast cells [138]:*

2 ml of YPD broth with yeast cells [77] was cultured until saturation or near saturation was reached. An OD<sub>600</sub> reading was taken and if the reading was above 3.0 then 5 ml of YPD broth per transformation was inoculated. The larger culture was grown to an OD<sub>600</sub> reading of 0.8-1.2. The cultures were then transferred into sterile 50 ml tubes and spun at 3,750 x g for 2 min at 4 oC, after centrifugation the supernatant was discarded, and the tubes placed on ice. The pellet was then resuspended in 10 ml of 1-step buffer (1:4 ratio of 0.2 M LiOAc and 40% (w/v) PEG 4000, respectively). The tubes containing the cell suspension were then centrifuged at 3,750 x g for 2 min at 4oC, the supernatant was then discarded, and the tubes placed back onto ice for ~1 min to allow any 1-step buffer remaining to collect at the bottom of the tube which was once again removed. 90  $\mu$ l of 1-step buffer per transformation was added. The pellet was then resuspended by vortexing, ensuring no clumps remained. 88  $\mu$ l of the cell suspension was then added to 1.5 ml sterile tubes containing 100  $\mu$ g of sheared salmon sperm DNA (Takara Bio Europe, France, cat. No. 630440) (pre-boiled in a 100 o C heat block for 5 min), 1  $\mu$ g of a chosen plasmid, 200 ng of another plasmid, 200 ng of an additional chosen plasmid. The tubes were then vortexed and incubated for 30 min at 42 o C before being placed on ice. The cells were centrifuged for ~10 s after which the supernatant was discarded. The cell pellet was resuspended in 200  $\mu$ l of sterile H<sub>2</sub>O. All of the cell suspension was spread over the surface of a synthetic media plate with the appropriate amino acids missing, this was determined by the plasmids. The SD plates were then incubated at 30 o C for ~ 5 d to allow the cells to grow into colonies.

#### 5.2.6 Acetate and replica plating:

To maintain the plasmid the cells grown on SD plates were replica plated. If more than 12 colonies were present and the growth medium was YPD the replica plating occurred on YPAC plates. IF the growth medium plate was synthetic media lacking specific appropriate nutrients than the replica plating occurred onto PSP2 plates. The replica plates were then incubated for ~48 h at 30 ° C to grow and the original transformation plates were also incubated and left to regrow. By matching the original plate to the PSP2 colonies which had grown on the PSP2 plate were then streaked onto streaked on synthetic media lacking appropriate nutrients and incubated for ~48 h at 30 °C. One colony from each newly streaked synthetic media plate were then streaked onto ~1/6 of a YPAC plate and incubated for ~48 h at 30 ° C. Any colonies which were unable to grow successfully on the YPAC plate were discarded.

### 5.2.7 Protein extractions for $\beta$ -galactosidase assays

The tubes were centrifuged at 12,000 X g for 1 min at room temperature and the supernatant was discarded. 100  $\mu$ l of ice-cold 1 x reporter lysis buffer (1 x RLB) (no. E3971; Promega, Southampton, United Kingdom) was added to each sample and the pellets were resuspended by vortexing. The cell suspension was then transferred to 2 ml flat-bottom screw cap tubes containing 150 mg of glass beads (Stratech cat. No. 11079105). The tubes were then homogenised in a Precellys 24 instrument at 6500 rpm for 3 cycles of 10 s, a 5 min break was taken between every cycle during which the cells were placed on ice to cool. After homogenisation 100  $\mu$ l of ice-cold RLB was added to each samples and the tubes were vortexed briefly. The tubes were then centrifuged at 12,000 X g for 2 min at 4 °C. The supernatant was then transferred into a screwcap tube, the protein lysates were then frozen in liquid nitrogen and stored at – 80 °C.

### 5.2.8 DC protein assay:

To quantify the concentration of protein in the protein extraction lysate a DC assay (Bio-Rad, Hemel Hempstead, UK, cat. No. #500-0113 and #500-0114) was performed. A bovine serum albumin protein standard was prepared in H<sub>2</sub>O with a range of concentrations; 62.5, 125, 250, 500, 1000 and 2000  $\mu$ g/ml. 5  $\mu$ l of each standard was added to a U-bottom well (two wells per standard). A dilution of 1:10 of the lysate using H<sub>2</sub>O was prepared and 5  $\mu$ l was added per well (two wells per sample). 25  $\mu$ l of DC assay reagent A (Bio-Rad #500-0113) was added to all wells followed by 200  $\mu$ l of DC assay reagent B (Bio-Rad #500-0114). The plates were then left for 15 min at room temperature, with gentle shaking (50 rpm), after which a Spectramax 190 plate reader was used to measure the absorbance at 750 nm.

### 5.2.9 $\beta$ -Galactosidase assay:

To assess the activity levels of  $\beta$ -galactosidase and therefore in turn assess the levels of UPRE-associated gene expression the  $\beta$ -galactosidase reporter assay kit (Promega, cat. No. E3971) was used. 1  $\mu$ l of 1 U/ $\mu$ l of  $\beta$ -galactosidase was added to 99  $\mu$ l ice-cold reporter lysis buffer (RLB), mixed, and then placed onto ice giving a 1:100 dilution. 10  $\mu$ l of the 1:100 dilution was then added to 900  $\mu$ l of ice-cold reporter lysis buffer, mixed, and then placed on ice to give a 1:10,000 dilution. A range of standards were then created using 0, 0.5, 1.0, 1.5, 2.0, 2.5, 3.0, 3.5, 4.0, 4.5 and 5.0 mU of  $\beta$ -galactosidase. Standards were diluted with RLB to achieve desired concentrations. The appropriate volume of RLB for each standard was added to each

well, followed by the required sample volume to give a total sample volume of 50  $\mu$ l. 50  $\mu$ l of 2X assay buffer (Table 1) was added to each sample containing well and the plate was then covered with parafilm and incubated for 30 min at 37 °C. After incubation, 150  $\mu$ l of Na<sub>2</sub>CO<sub>3</sub> was added to each well to stop the reaction. The plate was then read using a Spectramax 190 plate reader at a wavelength of 420 nm.

#### *5.2.10 Fluorescent confocal microscopy cell culture:*

Cells were grown in 4 ml precultures in 2% galactose, 1% raffinose lacking uracil, adenine and leucine. 20 ml of the same culture was inoculated with an initial OD<sub>600</sub> of 0.01 and grown overnight in the rotary incubator at 220 rpm and 30 °C. Cells were harvested the next day if the OD<sub>600</sub> value was between 0.5 and 0.8. Centrifugation of the samples was at 3000 x g for 2 min at 4 °C. The supernatant was discarded, and the cell pellets were resuspended in 1 ml of the same culture media. The cell suspension was transferred to a 1.5 ml microcentrifuge tube. 3  $\mu$ l of the cell suspension was placed onto a glass slide and the cover slip was then placed and sealed using nail polish. For stressed cells, DTT was added to the cell suspension at a concentration of 2 mM. The same slide preparation occurred for the stressed cells. The prepared slides were then imaged using the Zeiss LSM 880 with Airyscan confocal inverted light microscope (Zeiss Ltd, Cambridge, UK).

#### *5.2.11 Microscopy analysis:*

The Zeiss LSM 880 with Airyscan confocal inverted light microscope was set up using two channels, on channel detected the GFP signal and the other channel detected the mCherry signal. For the GFP signal the Ch1-T1 (photomultiplier tube) channel was used with an excitation wavelength of 488 nm, an emission wavelength of 523 nm and a detection wavelength of 523 nm. For the mCherry signal the Ch2 GaAsp-T2 (gallium arsenide phosphide detector) channel used an excitation wavelength of 594 nm, an emission wavelength of 611 nm and a detection wavelength of 611 nm. The objective used was the Plan-Apochromat 63x/1.4 Oil DIC M27 using the MBS 488/594 beam splitter. The laser power for the 488 nm laser was 4.5% and for the 594 nm laser the power was 56.8%. Gain settings were set to 880. All the microscope settings used here were reused for all images captured. Once the images had been captured, they were then Airyscan processed with an Airyscan strength of 7. Images were then analysed using ImageJ, individual cells were marked using ImageJ's ellipse tool as seen in Figure 2.A. To measure the fluorescence a manual threshold of 30, Figure 2B. Particles

greater than  $0.03 \mu\text{m}^2$  were then analysed. To calculate the fluorescence of the particles a background fluorescence reading was first taken. The background fluorescence reading was then subtracted from the fluorescence readings of the cell and particles. A set of images were taken at the 0 h timepoint with a slide of cells which had not been exposed to an ER stressor, but the time points which were after DTT addition were taken with a different slide of cells due to the slides being sealed. Therefore, the same cells used after DTT addition were not the same as the cells used without ER stressor.

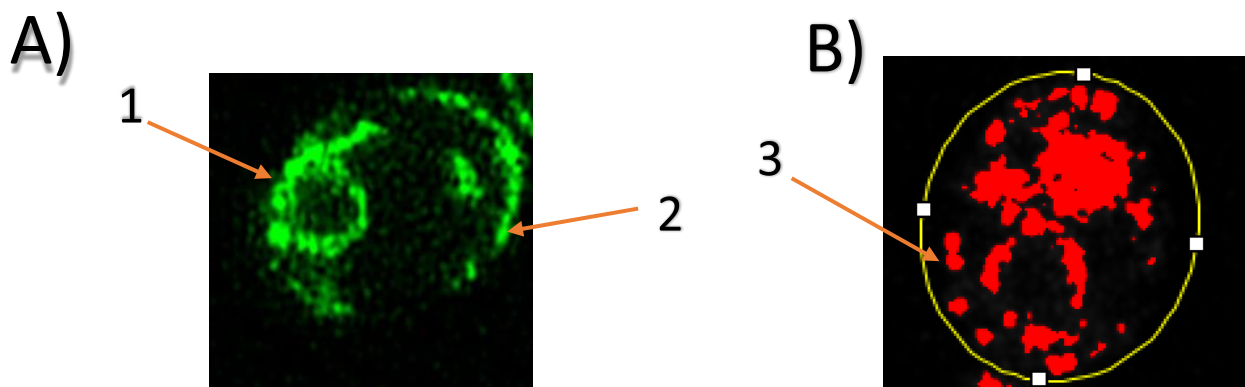


Figure 3. Individual cell selected with Image J ellipse tool (yellow ellipse). The cortical ER is indicated by arrow 1, the perinuclear ER is indicated by arrow 2 and a particle of mCherry is labelled with arrow 3. Part B displays a cell with the mCherry track with the manual threshold applied.

#### 5.2.12 Statistical analyses:

Experimental data were analysed using Prism 7 software (GraphPad Software Inc, La Jolla, California). Standard error of the mean (SEM) was calculated and for all data error bars represent the SEM, where statistical analysis has been performed. A 2-way ANOVA was used for all data testing to determine statistically significant differences,  $p < 0.05$ , between the means of the data. Both the Tukey test and Sidaks correction were used to correct for multiple comparisons and to adjust p values. The data for the  $\beta$ -galactosidase reporter assays and microscopy data was transformed using  $\log(Y+1)$  to satisfy the assumptions of the 2-way ANOVA as the compiled data had unequal variances when tested using the Brown-Forsythe test (Microsoft Excel). The  $\beta$ -galactosidase assays for Dcr2, H388A-DDCR2, PTC2 and E37A-D38A-PTC2 were completed in parallel and therefore these groups share the same control group data.

## 6.0 Results:

### 6.1 Characterising the effect of phosphatase overexpression on the induction of a UPR- $\beta$ -galactosidase reporter

#### 6.1.1 Rationale

The UPR must be negatively regulated by some mechanism because once the ER stress is removed the UPR returns to levels observed in unstressed cells [139]. A likely candidate for a negative regulator may be a phosphatase due to phosphorylation of Ire1 being a likely mechanism of activation. The chosen phosphatases have been previously investigated by Welihinda *et al.*, 1998, this study observed that a deletion of *ptc2* was able to sensitise cells to unfolded proteins and led to an increase in  $\beta$ -galactosidase activity. Welihinda *et al.*, 1998 also demonstrated that an overexpression of wildtype Ptc2 but not catalytically inactive was able to reduce reporter activity. In addition to this, Armstrong *et al.*, 2017 observed that overexpression of WT Ptc2 inhibited cell growth and deletion of *IRE1*, or the use of a mutant lacking phosphorylation sites were able to alleviate this effect. However, Armstrong *et al.*, 2017 also noted that activation loop mutants did not affect Ire1 inactivation suggesting that the previous hypothesis that Ptc2 may negatively regulate Ire1 by dephosphorylation may not be true. Therefore, this study aims to add further evidence for the role of Ptc2 as a negative regulator by investigating the effect of Ptc2 deletion and overexpression on the UPR through the use of a UPR  $\beta$ -galactosidase reporter assay. Dcr2 was first identified for its mitogenic properties [129] before further studies into Dcr2 suggested that it downregulates the UPR and that Dcr2 physically interacts with IRE1 [128]. Pathak *et al.*, 2007 also found that Dcr2 physically interacted with Sic1p and that overexpression of Dcr2 destabilised Sic1P suggesting that the physical interaction observed by Guo & Polymenis., 2006 between Dcr2 and Ire1 may lead to destabilisation of Ire1. Dcr2 was also investigated by Armstrong *et al.*, 2017 but unlike Guo & Polymenis., 2006 it was suggested to not affect the survival of ER stress. To further characterise the role of Dcr2 and Ptc2 and the effect they have on the activation of the UPR, the activation of the UPR was measured using a UPR-associated- $\beta$ -galactosidase reporter assay. Should Dcr2 or Ptc2 negatively regulate the UPR then reduced activation of the UPR would be observed.

The  $\beta$ -galactosidase-reporter assay works by hydrolysing *ortho*-nitrophenyl- $\beta$ -galactoside (ONPG) that is present in the 2X assay buffer used in the assay. The ONPG is

hydrolysed by the  $\beta$ -galactosidase enzyme which catalyses the hydrolysis of  $\beta$ -galactosides. The *E. coli* gene *lacZ* encodes  $\beta$ -galactosidase, the reporter is constructed so that *lacZ* uses the UPRE region from the *KAR2* which has been inserted upstream of a crippled *CYC1* promoter which in the absence of an upstream activating sequence is transcriptionally silent [140]. Therefore, when the UPR is induced during ER stress and *KAR2* is expressed, so too is *lacZ* due to them sharing the UPRE sequence. The  $\beta$ -galactosidase produced by the *lacZ* gene cleaves ONPG producing galactose which is colourless as well as nitrophenol which has a yellow colour. This allows for a measurement based on the change in colour, measured at 419 nm, and is a sign of reporter activity. Expression of the UPR-associated gene *KAR2* requires the translation of mature *HAC1* mRNA [48,90,141], therefore the Ire1 RNase domain must be active to complete *HAC1* mRNA splicing. In summary, a change in absorbance would indicate induction of UPRE-associated genes has occurred, which would also suggest RNase- and UPR-activation. To quantify this response, standardisation of the quantity of  $\beta$ -galactosidase to the total protein content was calculated using DC assays. The unit for this is mU of  $\beta$ -galactosidase per mg of total protein.

#### 6.1.2 Results for the $\beta$ -galactosidase reporter assay

To assess reporter activity 50 ml samples were taken at the 0 h time point and compared with 50 ml samples taken 1 h and 2 h after addition of 2 mM DTT. The wild-type cells gave an expected result with an increase in UPRE-*lacZ* activity over time with the largest difference being between the 0 h sample and the 2 h sample, Figure 4. It was observed that all strains lacking Ire1 gave very low levels of UPR activation, which was expected due to the  $\beta$ -galactosidase assay being based upon Ire1 splicing *Hac1* mRNA to induce UPRE-associated genes. There was no statistical difference, calculated by 2-way ANOVA, between  $\Delta dcr2$  cells and wild-type cells which suggests that loss of Dcr2 does not lead to an increase in UPR activation. The same was true for  $\Delta ptc2$  cells, they also lacked any statistical difference when compared to the baseline of the wild-type cells. This would suggest that the same that loss of the Ptc2 phosphatase is not sufficient to sensitise the UPR to ER stress. Both  $\Delta dcr2$  and  $\Delta ptc2$  in yeast cells also appear to lack the ability to sensitise the UPR to ER stress, as the levels of UPR expression were comparable between *dcr2* $\Delta$  *ptc2* $\Delta$  cells and the wild type. This implies

that in the absence of Dcr2 and/or Ptc2, Ire1 is able to induce UPR activity comparable to that observed in wild-type cell.

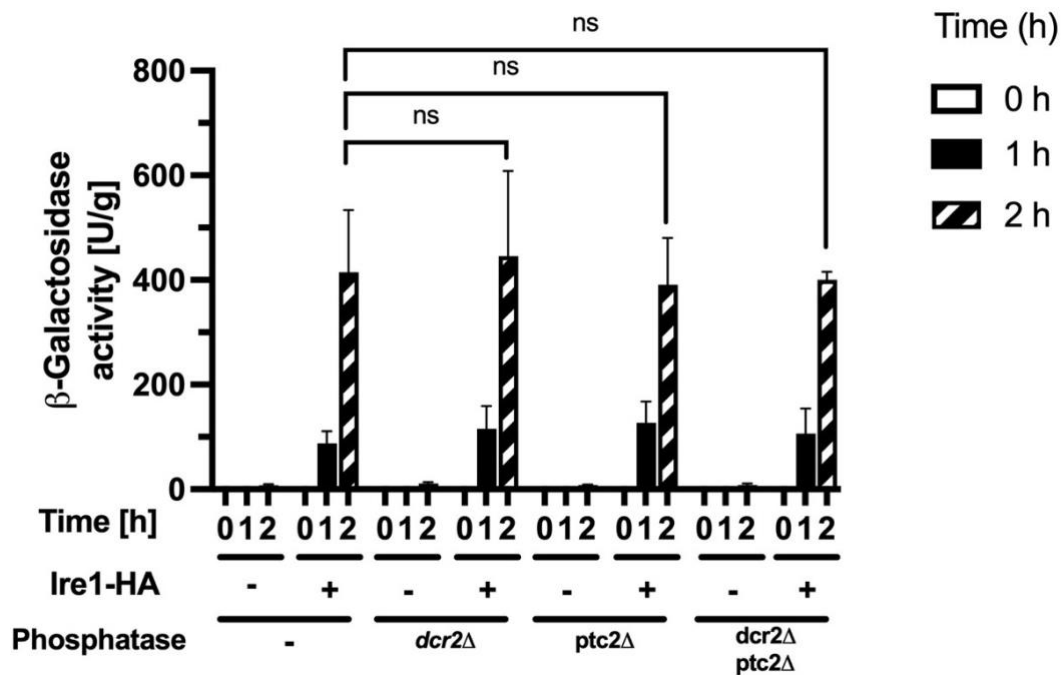


Figure 4. Phosphatase deletion strains. Bars represent standard errors (biological repeat of n=9 for wild-type and wild-type empty vector, all other samples have biological repeat of n=6). Significance determined by 2-way ANOVA.

Next the ability of the phosphatase Dcr2 to negatively regulate the UPR when overexpressed was investigated. Firstly, the strains lacking Ire1 when compared to their respective Ire1 containing strains had a much lower level of  $\beta$ -galactosidase activity at all time points, which was to be expected, Figure 5. Next was the comparison of overexpression of *DCR2* with the wild-type cells. Although, the amount of  $\beta$ -galactosidase activity may appear lower for the 2 h time point, when compared statistically using 2-way ANOVA there was no statistical difference between cells overexpressing *DCR2* and wild-type cells from the data gathered from six repeats. This would suggest that the Dcr2 phosphatase does not have the ability to negatively regulate the UPR on its own. This means that Dcr2 may be able to regulate the Ire1 and the UPR but only to a small extent. The catalytically inactive counterpart of Dcr2, H388A-DCR2, which still has the ability to bind to Ire1 [129] also appeared to have lower UPR activation at 2 h, but when compared statistically there was also no difference between the overexpression of *H388A-DCR2* and wild-type cells. The lack of statistical difference for both Dcr2 and H388A-DCR2 may be due to the data having a large standard deviation which may require additional repeats to reduce this, or there may be inherent variation in the

experimental design, such as the toxicity of phosphatase overexpression. H388A-DCR2 was investigated as well because it may have acted as a competitive inhibitor to the Dcr2 present in the cells. The same can be said for H388A-DCR2 overexpression as with the Dcr2. Comparison of the DCR2 mean, ~250 U/g, and the wild type mean of ~500 U/g would suggest a difference; however, this difference is not considered to be significant by 2-way ANOVA but does not confirm the opposite.

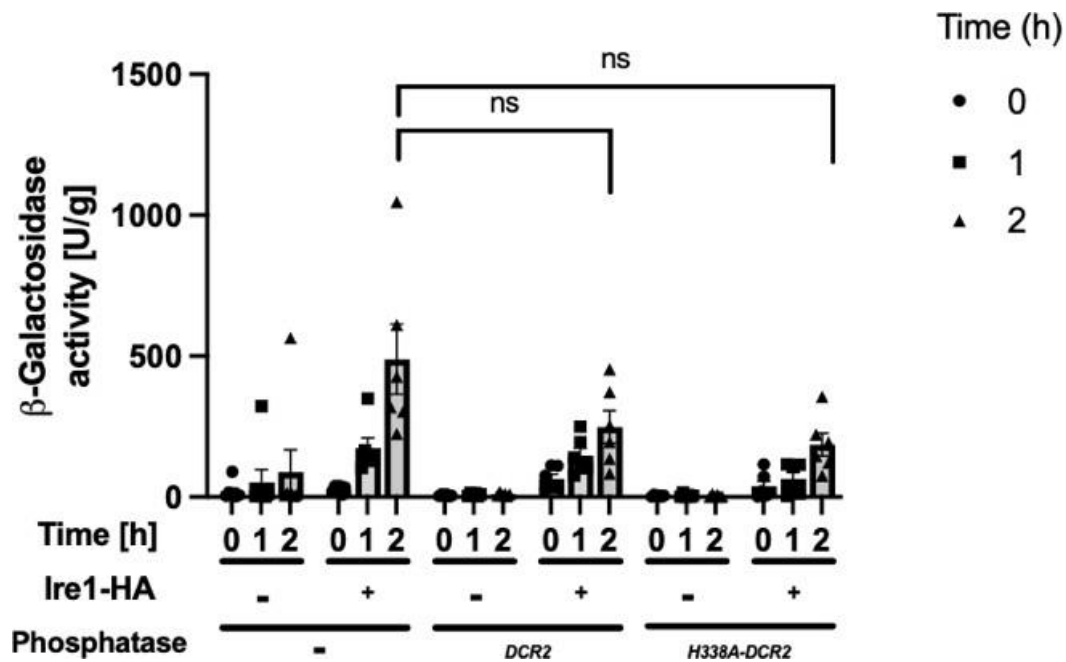


Figure 5.  $\beta$ -Galactosidase reporter assay for *DCR2* and *H338A DCR2* overexpression strains. Cells were grown to mid-exponential growth before collection. Bars represent standard errors (Biological repeat  $n=6$  for all strains). Significance determined by 2-way ANOVA. Assay completed in parallel with Figure 6 and therefore share the same control group.

The ability of the phosphatase *Ptc2* to negatively regulate the UPR when overexpressed was also investigated. Similarly, to Figure 5, the strains lacking *Ire1* when compared to their respective *Ire1* containing strains had a much lower level of  $\beta$ -galactosidase activity at all time points, Figure 6, which was to be expected. Next was the comparison of overexpression of *PTC2* with the wild-type cells, Figure 6. The  $\beta$ -galactosidase activity at the 2 h time point was lower for the *PTC2* overexpression strains when compared to the wild-type and was statistically different using 2-way ANOVA ( $p<0.05$ ), with data gathered from six repeats. This would suggest that the *Ptc2* phosphatase has the ability to significantly reduce the expression of the UPR on its own. The catalytically inactive counterpart of *Ptc2*, E37A-

D38A-PTC2, was also overexpressed in a separate strain but was not able to reduce the  $\beta$ -galactosidase activity to a point where it was statistically significant using 2-way ANOVA. This would suggest that the catalytic activity of Ptc2 is an important part of its regulation as its catalytically inactive counterpart was unable to cause a significant difference in UPR expression. This observation supports the hypothesis that the Ptc2 phosphatase is a negative regulator of the UPR.

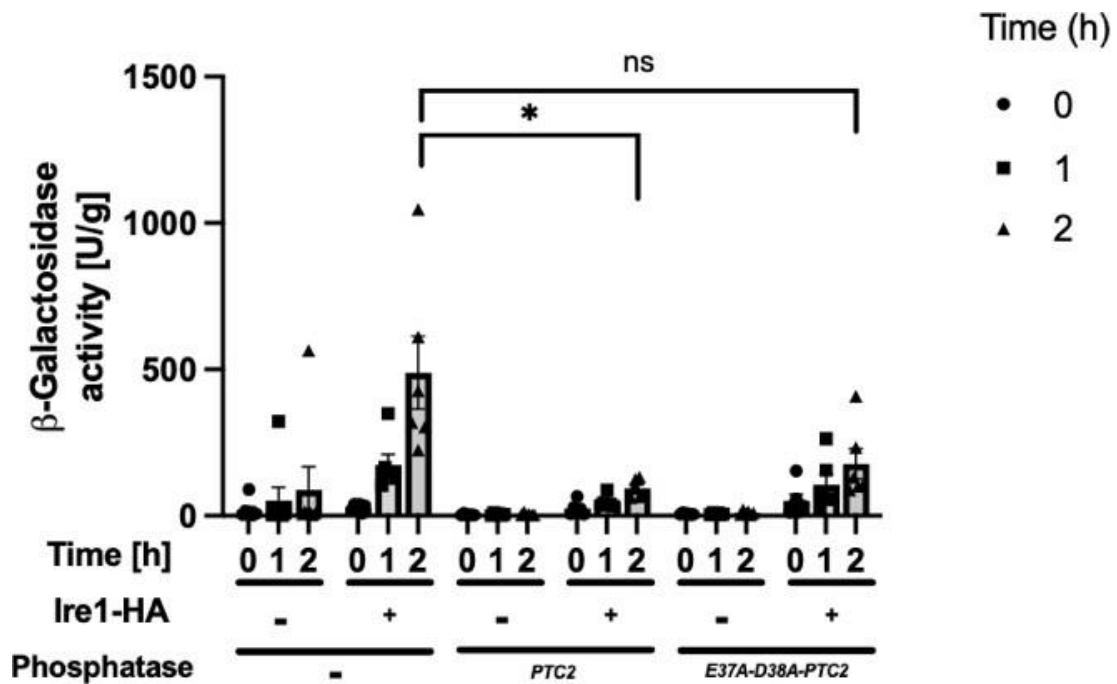


Figure 6.  $\beta$ -Galactosidase reporter assay for *PTC2* and *E37A D38A PTC2* overexpression strains. Cells were grown to mid-exponential cells before collection. Bars represent standard errors (Biological repeat  $n=6$  for all strains). Significance determined by 2-way ANOVA. Assay completed in parallel with Figure 5 and therefore the control group is shared.

## 6.2 Clustering of Ire1 in phosphatase overexpression mutants during ER stress

### 6.2.1 Rationale

When unfolded proteins accumulate in the ER and are detected by Ire1, Ire1 forms dimers and possibly oligomerises. How Ire1 clusters remains uncertain [26,48,142], but it is known that the Ire1 molecules do cluster during ER stress. Once overexpression of the phosphatases has been demonstrated to reduce expression of the UPR-*lacZ* reporter then the mechanism by which the UPR is negatively regulated can be investigated through the use of the phosphatases. One mechanism may be the prevention of Ire1 clustering which is a sign that the ER stress response has been initiated [48,134]. If a reduction in clustering is observed, either by reduced numbers of particles or a reduced fluorescence intensity, then this would

suggest that the phosphatases interfere with clustering of Ire1. Ptc2 gave a significant

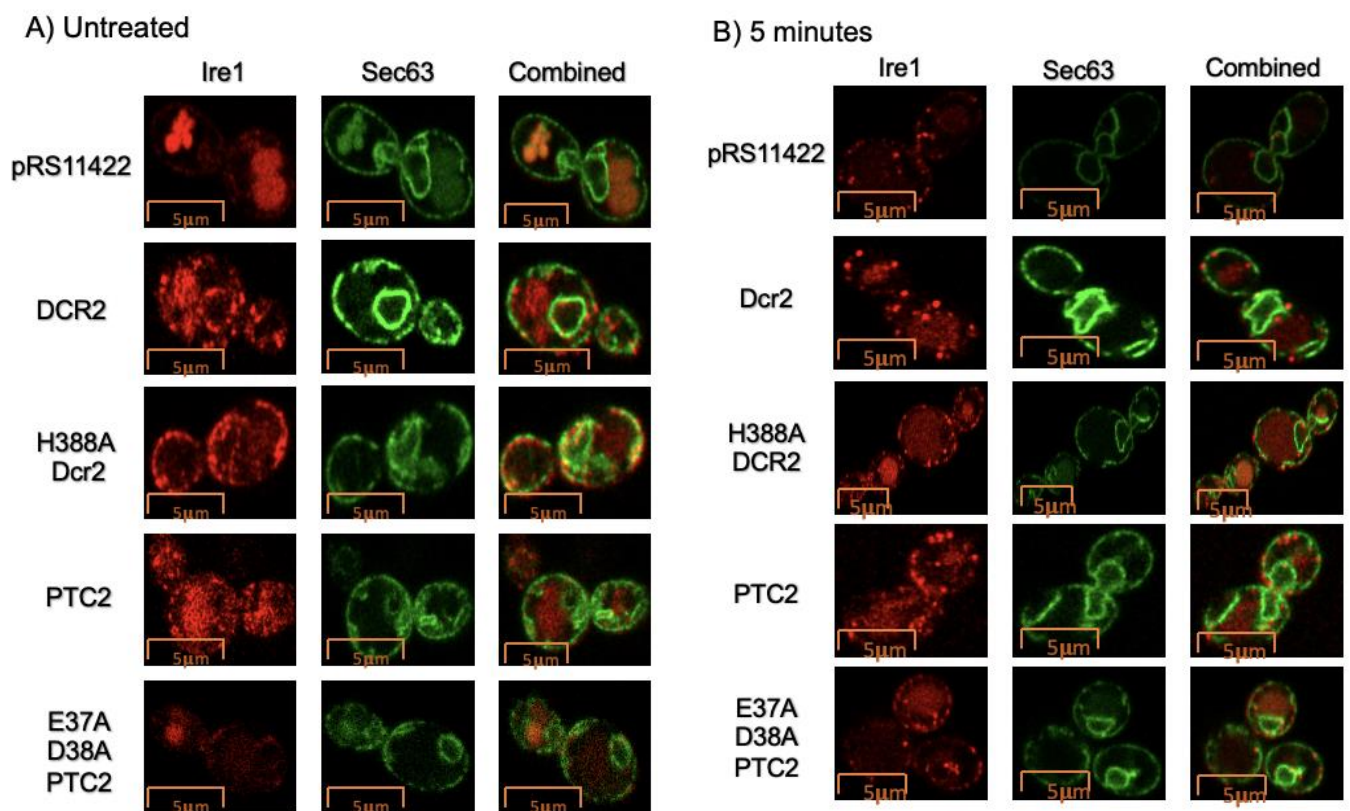
difference in the *β-galactosidase* assays suggesting Ptc2 is a negative regulator and therefore warrants continued investigation. In contrast to Ptc2, Dcr2 was not able to produce a significant change in expression of the UPR-*lacZ* reporter, which would suggest that Dcr2 is not a negative regulator. However, Dcr2 was continued to be investigated as previous work has suggested a physical interaction between Dcr2 and Ire1, this interaction may then cause a change in the clustering of Ire1. The change in foci formation may not lead to a significant reduction in UPR signalling as shown by the lack of effect in the UPR-*lacZ* reporter but any changes in foci formation such as change in particle number or a change in the fluorescence of particles may still suggest an interaction between Dcr2 and Ire1.

To investigate clustering by Ire1 after activation a *S. cerevisiae*  $\Delta$ ire1 strain, was transformed with three plasmids. The first plasmid is pJK59 which includes the GFP-tagged Sec63 so that the cortical and perinuclear ER can be visualised for determining the location of Ire1. The second plasmid was pEvA97 which contained *IRE1* with the mCherry fluorescent tag, this allowed the localisation of Ire1 to be visualised. The third plasmid was pRSII422 which contained either DCR2, H338A-DCR2, PTC2, E37A-D38A-PTC2 or no insert. Using a Zeiss LSM 880 with Airyscan microscope, images were collected over five time points, 0 min, 5 min, 15 min, 30 min and 60 min after induction of ER stress with 2 mM DTT. If there is not a defect in Ire1 clustering than clustering of Ire1 using the mCherry signal should be clear.

### 6.2.2 Confocal microscopy results

A 2-channel approach was used to ensure visualisation of cells expressing Ire1 and Sec63. In addition to this, cells were only chosen for imaging if both the mCherry signal from Ire1 and the GFP signal from Sec63 were detectable. In cells where ER stress had not been induced, there should be no specific *foci* formation sites as the UPR is not activated [48]. Ire1 should be spread evenly along both the cortical and perinuclear ER membrane. The introduction of ER stress from DTT should not affect the ER membrane distribution of Sec63, the GFP-tagged Sec63 should allow visualisation of where the Ire1-mCherry is localised to. The localisation of Ire1-mCherry can be observed in Figure 6. The mCherry signal is mainly localised to the cortical and perinuclear ER, Figure 6A, however it is not an even distribution as can be seen in Figure 5A. mCherry fluorescence can also be seen in the body of all investigated strains before the induction of ER stress, Figure 6.

The clusters that Ire1 forms during ER stress can be seen from the 5 min time point, Figure 6B. The clusters become clearer with the Ire1 becoming less spread along the ER from the 15 min timepoint, Figure 6C. The clustering of the Ire1 produces a stronger mCherry signal due to the increased amount of mCherry-tagged Ire1 in once location. To demonstrate that all mutants share the same phenotype, the same characteristics should be seen in the mutants as in the wild type. Around 4 images were taken per mutant per time point, with each image containing between 2-6 cells. The images collected from the microscopy show Ire1 clustering along the ER membrane, however, just because *foci* formation has been observed does not mean the downstream components of Ire1 signalling such as RNase activity has been induced.



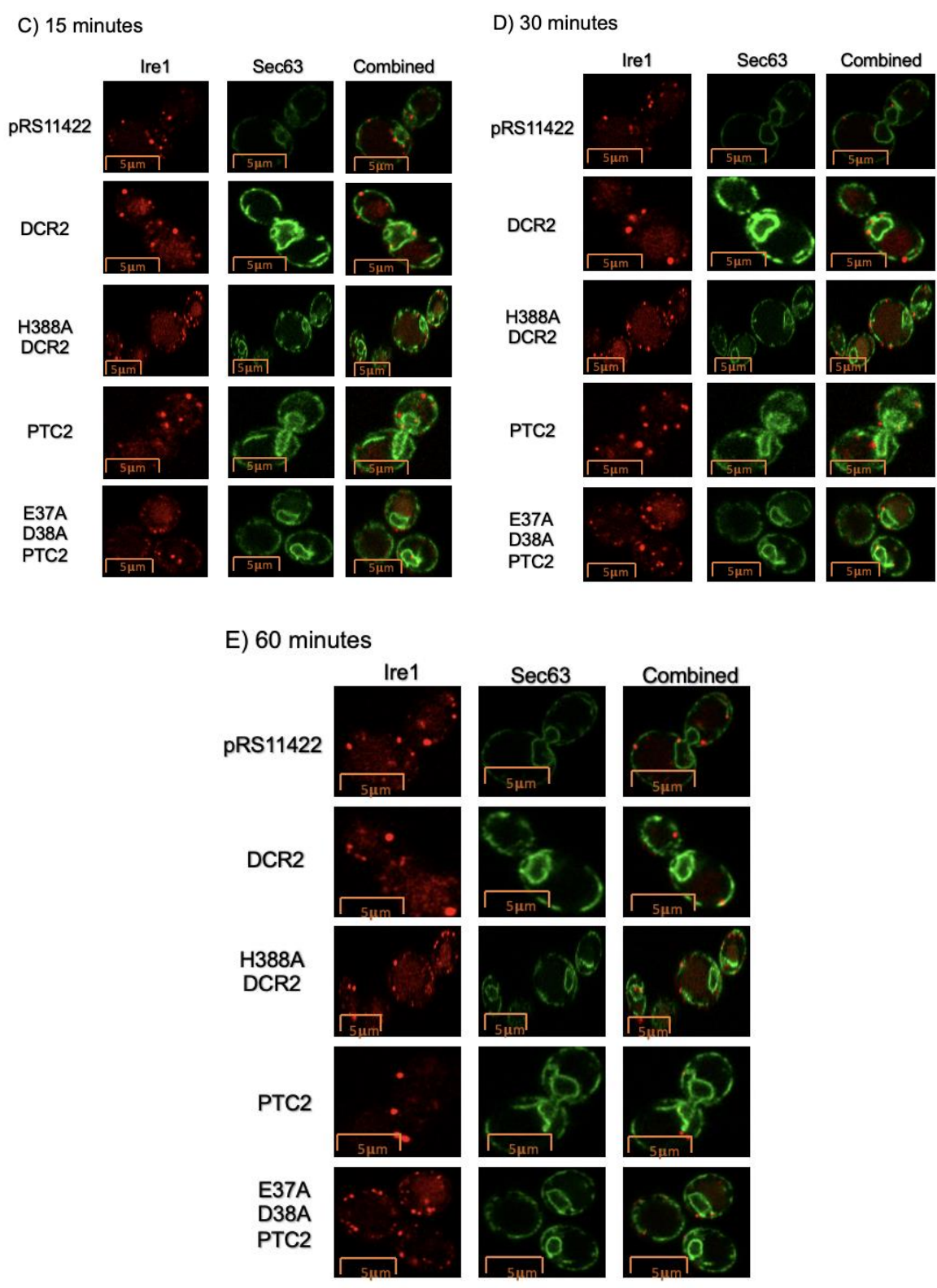


Figure 6. Fluorescence confocal microscopy with Airyscan. The 0 min time point of the different genotypes. There is an even distribution of GFP around the outer- and perinuclear membranes. The distribution of mCherry does not have a clear even distribution

The effect of the phosphatases Dcr2 and Ptc2 on the clustering of IRE1 was also investigated using confocal microscopy and mCherry-tagged IRE1. Upon ER stress Ire1 is known to oligomerise, therefore investigating the ability of Ire1-mCherry to form particles may be an indication of UPR activation. Previous studies have suggested phosphorylation sites are not required in the inactivation of Ire1 [49], hence negative regulation of Ire1 may be through interference of foci formation by Ire1 monomers. A previous investigation into the effects of phosphorylation mutants by Armstrong *et al.*, 2017 also suggested that phosphorylation mutants in the activation loop were unable to effect Ire1 clustering. It may then be expected that the phosphatases have no effect on the clustering as well, however, the investigation by Armstrong *et al.*, 2017 was only qualitative and only phosphorylation sites in the activation loop were investigated, this still leaves other phosphorylation sites such as in the  $\alpha$ EF insertion loop for the phosphatases to act on [80] There is a strong significant difference between the number of particles in wild-type cells at 60 min and *DCR2* as well as *H388A-DCR2* overexpressing cells at 60 min, Figure 7A. There is also a strong significant difference between the number of particles in wild-type cells at 30 and 60 min and *PTC2* overexpressing cells at 30 and 60 minutes, Figure 6B. However, comparison of cells overexpressing the catalytically inactive Ptc2 counterpart, *E37A-D38A-PTC2*, had no difference at the 60 min time points, Figure 7B. Both Dcr2 and Ptc2 were able to significantly decrease the number of particles formed which may suggest these negative regulators interfere with foci formation, whereas Ptc2 was able to reduce the number of particles formed at the 30 min time point which Dcr2 was unable to do, Figure 7. However, number of particles alone is not enough to draw strong conclusions as other factors such as the fluorescence intensity, which is an indication of mCherry tagged Ire1 monomers, may also affect the data.

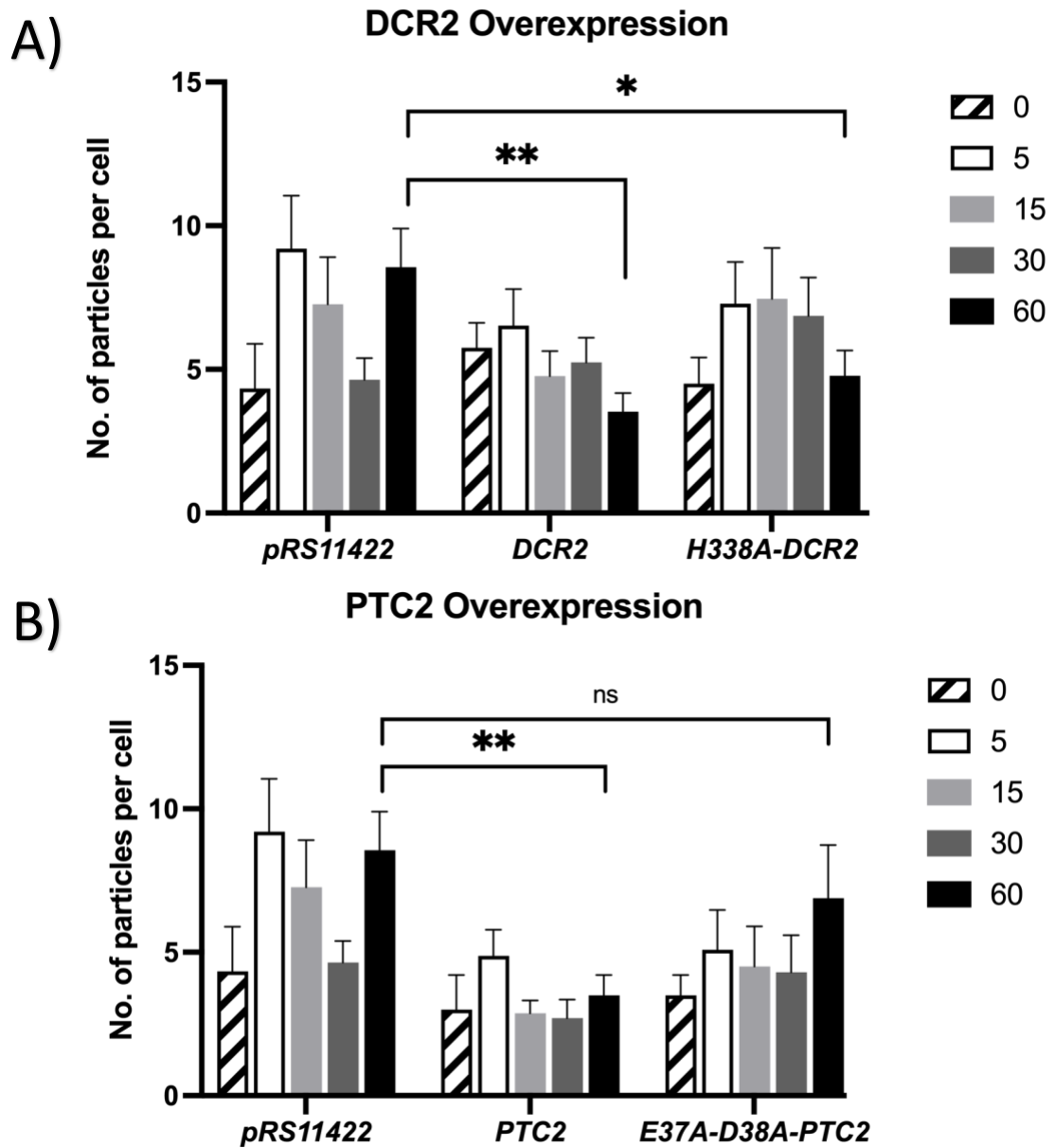
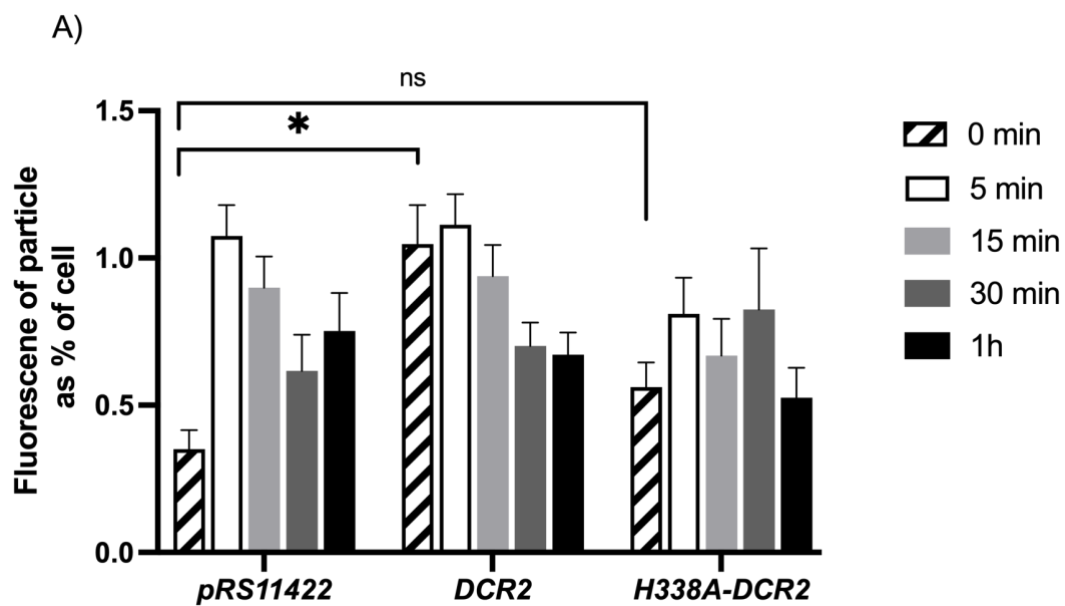


Figure 7. The number of particles per cell visible using Airyscan fluorescence confocal microscopy. Particles above  $0.03 \mu\text{m}$  were counted in wild-type cells (pRS11422) and in cells overexpression *DCR2*, the catalytically inactive *Dcr2* counterpart *H388A-DCR2* (A). Overexpression of *Ptc2* and its catalytically inactive counterpart *E37A-D38A-Ptc2* were also investigated (B) Images were taken at 5, 15, 30 and 60 min after the cellular stressor DTT was added and an image was taken before the stressor was added. \* Represents a p-value of  $\leq 0.05$ . Significance determined by 2-way ANOVA

To further investigate the effect of Ptc2 and Dc2 overexpression on Ire1 clustering the fluorescence intensity of the particles in the cells was measured. The fluorescence intensity of the particles may be a better measure of Ire1 clustering than the number of particles in cells alone. This is in part due to the mechanism by which the Ire1 clusters form being unknown. The fluorescent mCherry is directly tagged onto the Ire1 protein therefore an increase in intensity would suggest that there is a greater amount of Ire1 in the particle. There is a strong significant difference between the Dcr2 overexpression and the wild-type cells before DTT was added, this suggests that the Dcr2 overexpressing cells were already undergoing stress possibly from the Dcr2 overexpression causing toxicity, Figure 8A. There were no other significant differences between the H338A-Dcr2, Ptc2 or E37A-D38A-Ptc2 overexpressing strains and the wild type cells, Figure 8. This may suggest that Ire1 and the UPR is not negatively regulated by interference with the foci formation of Ire1.



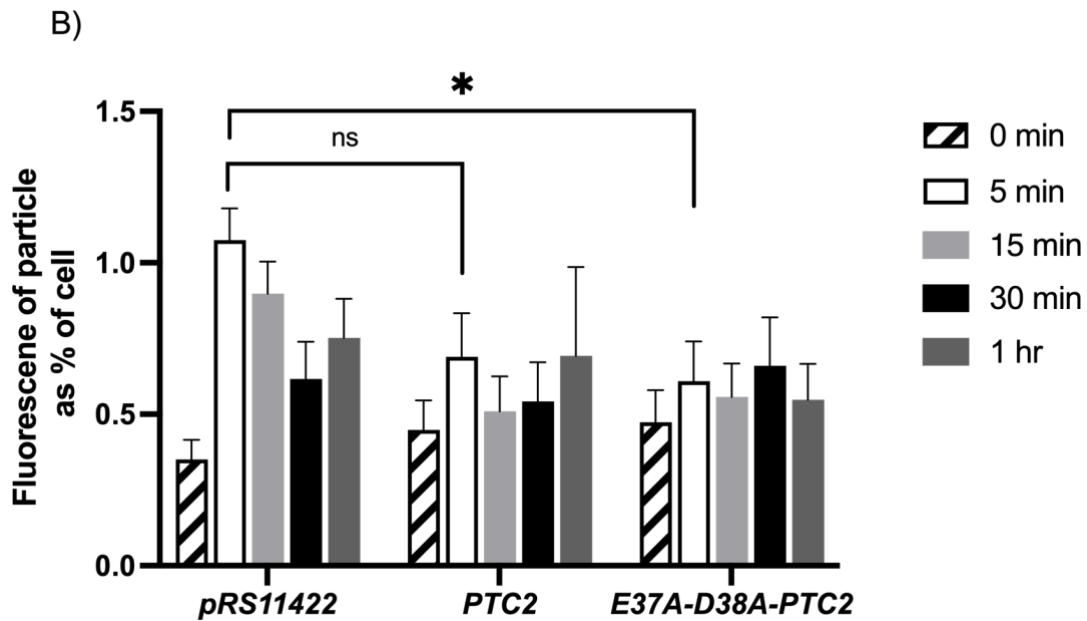


Figure 8. Fluorescence of particles as a percentage of the cell's fluorescence for both *Dcr2* (A) and *Ptc2* (B) overexpressing cells. Background levels of fluorescence were taken and subtracted from fluorescence of the cell and particles. Images were taken at 5, 15, 30 and 60 minutes after the cellular stressor DTT was added and an image was taken before the stressor was added. \* Represents a p-value of 0.05. Significance determined by 2-way ANOVA

## 7.0 Discussion:

The mechanism of inactivation for the UPR in both yeast and mammalian cells remains unknown. This study aims to further characterise the roles of two previously reported negative regulators of the UPR and investigate the mechanism by which they regulate.

### 7.1 Overexpression of phosphatases on UPR activation during ER stress conditions:

Previous work on *Ptc2* by Welihinda *et al.*, 1998 observed that loss of *Ptc2* sensitised cells and gave an increased *UPRE-lacZ* reporter assay and that overexpression caused a reduction in activity. In addition to the previous investigation, additional studies on *Ptc2* demonstrated that overexpression of *Ptc2* in cells which had all phosphorylation sites in the *Ire1* activation loop blocked was still able to negatively regulate the UPR [49]. To re-investigate the previously proposed phosphatases, *Dcr2* and *Ptc2*, both phosphatases were individually overexpressed as well as catalytically inactive counterparts for both phosphatases. A  $\beta$ -galactosidase reporter assay demonstrated that overexpression of *Ptc2* reduced  $\beta$ -galactosidase activity to a significant level when compared with wild-type cells, supporting previous evidence that *Ptc2* is negatively regulating the UPR, Figure 6. A significant difference was not observed in cells overexpressing the catalytically inactive counterpart of *Ptc2*, *E37A-*

D38A-Ptc2, suggesting that the catalytic activity was necessary for negative regulation of the UPR and the significant difference to be observed. In contrast, Dcr2 overexpression was not observed to give a significantly different effect on the  $\beta$ -galactosidase assays suggesting that Dcr2 may not be a negative regulator of the UPR and Ire1. There was a large spread of data around the mean for Dcr2 at the 2 h with the highest data point having a  $\beta$ -galactosidase activity value of  $\sim 500$  U/g. Whereas the Ptc2 dataset was highly consistent with little variation around its mean. Welihinda *et al.*, 1998 observed sensitisation of cells lacking Ptc2 to ER stress, however, this was not observed in this study. A reduction in the UPR-*lacZ* reporter was observed when Ptc2 was overexpressed which is in agreement with previous work [133]. For the Dcr2 overexpression  $\beta$ -galactosidase assay the data also agreed with previous work by Armstrong *et al.*, 2017 in which they observed that overexpression of Dcr2 had no impact on cell survival during ER stress. This may suggest that Dcr2 is not the main phosphatase involved in dephosphorylation of Ire1 and the UPR but that the relationship between Ire1 and Dcr2 is different than that of Ire1 and Ptc2.

#### 7.2 Foci formation by Ire1 is reduced in DCR2 and PTC2 overexpressing cells:

Previous work by Armstrong *et al.*, 2017, demonstrated that inactivation occurs in the absence of available phosphorylation sites, therefore an alternative mechanism of inactivation must be present. One alternative mechanism may be through interference Ire1 cluster formation, to investigate this confocal microscopy using mCherry-tagged Ire1 was used. To evaluate clustering both the number of particles and the fluorescence of the particles per cell were used. The number of particles for both *DCR2* and *H388A-DCR2* were significantly decreased only at the 60 min time point, figure 7A. This differs to the  $\beta$ -galactosidase assays for *DCR2* and *H338A-DCR2* where no decrease in activity was observed. However, the interpretation of particles per cell remains difficult due to the mechanism of foci formation being unknown.

Overexpression of *PTC2* at the 60 min time point significantly reduced the number of particles per cell compared with the control. However, a clear link between the number of particles and induction of UPR signalling has not been made. The *E37A-D38A-PTC2* mutant was not significant at any of the time points investigated, figure 7B. The variation in the results may be due to the different methods of recording. The  $\beta$ -galactosidase activity is a direct reporter of IRE1 activity as the *lacZ* is under control of the UPR target promoter region, UPR.

This means that the results from the  $\beta$ -galactosidase are an indication of direct IRE1 activation as it does not measure the activity of *HAC1* splicing or any targets of the active Hac1 protein. Whereas the confocal microscopy is only a “snapshot” of a few cells out of a larger culture, particles were also observed in “unstressed” cells with a varying number of particles in cells with the same genotype. A resolution to the “snapshot” would be to image a greater number of cells to confirm the observation is seen in a large portion of the cells. There is clustering of mCherry visible at the 0 h time points of the confocal images, this small amount of clustering appears in cells that are “unstressed” as even healthy cells have low levels of UPR activation to alter the folding capacity of the cell which is closely linked to the metabolic state of the cell [22]. It has been observed in previous studies of *Ptc2* that overexpression of wild type *Ptc2* was able to inhibit growth of cells [133], the addition of DTT in this study further affected cells overexpressing *PTC2* suggesting that overexpression of *PTC2* may lead to a dysregulated UPR. This may explain the difference between the  $\beta$ -galactosidase assays and the confocal microscopy when comparing the phosphatases to the wild-type cells.

Measuring the number of particles per cell is only an indication of clustering as it lacks the ability to distinguish the size of the particles and the number of Ire1 monomers that may have clustered. Therefore, quantification of the fluorescence of each particle offers a greater quantitative method for determining Ire1 clustering. The method works on the principle that the greater the fluorescence of a particle then there is a greater number of mCherry-tagged Ire1 monomers present in that particle. Cells overexpression of *Ptc2* or E37A-D38A-*PTC2* demonstrated no significant difference from wild-type cells, Figure 8. In contrast to this, overexpression of *Dcr2* showed a significant difference, however, this difference was only observed at the 0 h time point, Figure 8. The difference between the wild-type and *Dcr2* overexpressing cells was that the particles at the 0 h time point had a much greater fluorescence than that of the wild-type, the levels of fluorescence were similar to that of the wild-type at the 5 min time point, Figure 8. This would therefore suggest that the *Dcr2* cells are undergoing stress possibly due to the overexpression of the *Dcr2*, this difference was not observed for any of the other phosphatases. This increase in fluorescence for cells overexpressing *Dcr2* before any stressor has been added is also consistent with other data from the Schroeder laboratory where activation of the *UPRE-lacZ* reporter activity was seen before addition of DTT to cells. This may further confirm that overexpression of *Dcr2* can

cause stress to the cell leading to UPR signalling being active before addition of stressors. The confocal fluorescence data suggests that the mechanism of action of the phosphatases is not through interference with Ire1 clustering as no phosphatases was able to cause a significant decrease in fluorescence suggesting that the wild-type amount of Ire1 was gathered during foci formation. The image quality of the cells at the 0 h time point are also not as clear as those at later time points, these images would need to be repeated so that equally clear pictures are available throughout the 60 minute time frame.

## 8.0 Conclusion and future work:

### 8.1 Summary of findings

To summarise the findings of this paper, the Ptc2 phosphatase was able to reduce  $\beta$ -galactosidase activity when overexpressed, however, Dcr2 overexpression as well as both catalytically inactive counterparts E37A-D38A-PTC2 and H338A-DCR2 were unable to significantly effect  $\beta$ -galactosidase activity. Previous work by Armstrong *et al.*, 2017 suggested that phosphorylation may not play a role in the inactivation of Ire1, therefore this study investigated interference of Ire1 clustering as an alternate mechanism of regulation. This study found no significant differences between the fluorescence of mCherry particles of wild-type and phosphatase overexpressing cells.

Results from the  $\beta$ -galactosidase assays agree with work done by Welihinda *et al.*, 1998 and Armstrong *et al.*, 2017 that Ptc2 acts as a negative regulator of the UPR. It also adds evidence to previous work by Armstrong *et al.*, 2017 that Dcr2 does not negatively regulate the Ire1 and the UPR. The ability of Ptc2 overexpression to lower activation of the UPR-*lacZ* reporter does not however confirm the mechanism by which Ptc2 regulates Ire1. Ptc2 also inhibits transcription of genes not under control of Hac1, which leads to the possibility that attenuation of UPR signalling is caused by attenuation of transcription and not direct attenuation of UPR signalling through interactions with Ire1. The use of activation loop mutants would have been able to expand on the results of this study as the importance of activation loop phosphorylation would also have been elucidated. If overexpression of Ptc2 on the phosphorylation mutants gave no significant difference for the UPR-*lacZ* reporter assay than from the observations in this study, it would have suggested that Ptc2 acts through the phosphorylation loop. If the activity of the UPR-*lacZ* reporter was still reduced than the

phosphorylation sites in the activation could have been excluded as the target of Ptc2 regulation, however, phosphorylation sites in the  $\alpha$ EF insertion loop are still present so dephosphorylation cannot be ruled out.

Investigation into the possibility that Ptc2 interferes with foci formation of Ire1 was also conducted using confocal microscopy. If interference of Ire1 clustering was the mechanism by which Ire1 is negatively regulated then a reduction in fluorescence would be expected, however, no effect on IRE1 foci formation was observed during stress when overexpressed phosphatases were present. There was also no difference between the cells overexpressing Dcr2 and the wild type when the stressor was added. However, Dcr2 overexpressing cells had increased levels of fluorescence at the 0 h time period when no cell stressor was present suggesting that overexpression itself was causing stress to the cell from possible toxicity of the phosphatase. These findings therefore suggest that a different mechanism of action than foci formation interference is responsible for negative UPR regulation by Ptc2, such as through a reduction in the levels of multiple mRNAs. The clustering results also adds further evidence that even if Dcr2 does physically interact with Ire1 as previously suggested [128] the interaction does not negatively influence Ire1 formation or UPR signalling.

## 8.2 Future work

### 8.2.1 Identifying phosphorylation state

As previously mentioned in this study, phosphorylation loop mutants have been previously investigated to evaluate the importance of phosphorylation in the activation and inactivation of IRE1 and the UPR [49]. It had been suggested that because *HAC1* splicing still occurs when all phosphorylation sites on the phosphorylation loop had been mutated that phosphorylation may not be solely responsible for activation of IRE1 [49]. In addition to this, loss of phosphorylation sites was shown to not effect inactivation suggesting that dephosphorylation is not necessary for inactivation [49]. To investigate the role of phosphorylation in the activation and inactivation of IRE1 phos-tag SDS-PAGE may have been proven to be a useful method. This method of SDS-PAGE allows for differentiation of non-phosphorylated proteins and they phosphorylated counterparts [143]. Therefore, using this method the phosphorylation state of IRE1 could be investigated before and after ER stress is instigated. However, even if a change in phosphorylation state is observed, using this method

it is not possible to dismiss other mechanisms of action such as a reduction in levels of mRNA which may be taking place at the same time. Hence this method would only be able to indicate if a change in phosphorylation state has occurred during activation or inactivation.

#### *8.2.2 Utilising activation-loop mutant strains:*

Additional experiments that may have furthered the results gathered in this study may have been to use the phosphorylation mutants created by Armstrong *et al.*, 2017. The study used wild type Ire1 cells alongside mutant strains with mutations in phosphorylation loop of the activation segment. The mutant strains consisted of: S840A S841A T844A S850A (termed Q-A) and S837A S840A S841A T844A S850A (termed P-A). A hierarchy to the importance of the phosphorylation sites was observed, with the S840 and S841 being considered more important [49]. A hierarchy of importance seems likely as previously stated in this study there are primary and secondary phosphorylation sites in some protein kinases with the primary site having greater importance [73]. Armstrong *et al.*, 2017 observed that these mutations did not cause any effect on the inactivation kinetics of IRE1 which suggested that dephosphorylation may not be the mechanism by which Ire1 is inactivated and prompted the investigation into foci formation by this study. By utilising these strains alongside the negative regulator phosphatases, which in this study was demonstrated to be Ptc2 due to its significant reduction on  $\beta$ -galactosidase activity, the importance of the activation loop in inactivation could have been investigated. If a reduction in the ability of Ptc2 to negatively affect  $\beta$ -galactosidase activity was seen when using either the QA or PA mutant strain then it would suggest that the Ptc2 acts through the activation loop of Ire1. In addition to this, if the PA strain but not the QA strain was observed to have this effect then the specific residues of the activation loop that contribute to inactivation could be further identified.

#### *8.2.3 Test cumulative effect of overexpressing both phosphatases*

In addition to utilising different Ire1 mutant strains, overexpression of both phosphatases may have been useful. This is because multiple phosphatases may contribute to the negative regulation of Ire1 and the UPR. Therefore, by overexpressing both phosphatases a significant difference may be observed that would have been too small to see in strains overexpressing each phosphatase alone. However, this is dependent on the relationship of the phosphatases and the sites they dephosphorylate. If the phosphatases share a phosphorylation site then the overexpression of both may be redundant. If the

relationship of the phosphatases was not redundant then during  $\beta$ -galactosidase assays this would manifest itself as an increased reduction in activity levels then either phosphatase was able to achieve alone. If this was observed this would indicate a hierarchy in the regulators of the UPR with certain regulators contributing a greater amount to inactivation than the other.

#### 8.2.4 Investigation into mRNA reduction as the mechanism of action

Finally, the use of northern blots may provide evidence for mRNA level reduction mechanism of action. *HAC1* mRNA becomes spliced upon activation of the UPR and then translated, the Hac1 protein then targets multiple genes such as *KAR2* and *PDI1* which help to alleviate the unfolded protein burden in the ER [90,141]. By investigating the effect of Ptc2 overexpression on the mRNA levels of these genes, the mechanism by which Ptc2 regulates the UPR may be identified. The inclusion of *KAR2* and *PDI1* as well as *HAC1* in the northern blots would be advantageous. This is because Ptc2 may not directly reduce the levels of *HAC1* mRNA but act at a later stage of the UPR where the targets of the *HAC1* protein become upregulated. This would be observed as there being no reduction in the *HAC1* mRNA levels but a reduction in *KAR2/PDI1* levels. If Ptc2 were to work at an earlier step and reduce the levels of *HAC1* this would be observed as a reduction in all three gene mRNA levels as a reduction in *HAC1* would lead to a reduction in *KAR2/PDI1*. By using this not only the possible mechanism of action would be revealed but it may also reveal which stage of the UPR is being regulated.

## 9.0 References:

1. Naidoo, N. ER and aging—protein folding and the ER stress response. *Ageing research reviews* **2009**, *8*, 150-159.
2. Chakrabarti, A.; Chen, A.W.; Varner, J.D. A review of the mammalian unfolded protein response. *Biotechnol Bioeng* **2011**, *108*, 2777-2793, doi:10.1002/bit.23282.
3. Read, A.; Schröder, M. The Unfolded Protein Response: An Overview. *Biology* **2021**, *10*, 384.
4. Kozutsumi, Y.; Segal, M.; Normington, K.; Gething, M.-J.; Sambrook, J. The presence of malformed proteins in the endoplasmic reticulum signals the induction of glucose-regulated proteins. *Nature* **1988**, *332*, 462-464.
5. Sidrauski, C.; Walter, P. The transmembrane kinase Ire1p is a site-specific endonuclease that initiates mRNA splicing in the unfolded protein response. *Cell* **1997**, *90*, 1031-1039.
6. Travers, K.J.; Patil, C.K.; Wodicka, L.; Lockhart, D.J.; Weissman, J.S.; Walter, P. Functional and genomic analyses reveal an essential coordination between the unfolded protein response and ER-associated degradation. *Cell* **2000**, *101*, 249-258.
7. Urano, F.; Wang, X.; Bertolotti, A.; Zhang, Y.; Chung, P.; Harding, H.P.; Ron, D. Coupling of stress in the ER to activation of JNK protein kinases by transmembrane protein kinase IRE1. *Science* **2000**, *287*, 664-666.

8. Shen, X.; Ellis, R.E.; Lee, K.; Liu, C.-Y.; Yang, K.; Solomon, A.; Yoshida, H.; Morimoto, R.; Kurnit, D.M.; Mori, K. Complementary signaling pathways regulate the unfolded protein response and are required for *C. elegans* development. *Cell* **2001**, *107*, 893-903.
9. Anfinsen, C.B.; Haber, E.; Sela, M.; White Jr, F. The kinetics of formation of native ribonuclease during oxidation of the reduced polypeptide chain. *Proceedings of the National Academy of Sciences of the United States of America* **1961**, *47*, 1309.
10. Stevens, F.J.; Argon, Y. Protein folding in the ER. In *Proceedings of the Seminars in cell & developmental biology*, 1999; pp. 443-454.
11. Jaenicke, R. Protein folding: local structures, domains, subunits, and assemblies. *Biochemistry* **1991**, *30*, 3147-3161.
12. Lévy, F.; Gabathuler, R.; Larsson, R.; Kvist, S. ATP is required for in vitro assembly of MHC class I antigens but not to transfer of peptides across the ER membrane. *Cell* **1991**, *67*, 265-274.
13. Dobson, C.M. Protein folding and misfolding. *Nature* **2003**, *426*, 884-890.
14. Hardesty, B.; Kramer, G. Folding of a nascent peptide on the ribosome. **2000**.
15. Bukau, B.; Horwich, A.L. The Hsp70 and Hsp60 chaperone machines. *Cell* **1998**, *92*, 351-366.
16. Hartl, F.U.; Hayer-Hartl, M. Molecular chaperones in the cytosol: from nascent chain to folded protein. *Science* **2002**, *295*, 1852-1858.
17. Schiene, C.; Fischer, G. Enzymes that catalyse the restructuring of proteins. *Current opinion in structural biology* **2000**, *10*, 40-45.
18. Hammond, C.; Helenius, A. Quality control in the secretory pathway. *Current opinion in cell biology* **1995**, *7*, 523-529.
19. Kaufman, R.J.; Scheuner, D.; Schröder, M.; Shen, X.; Lee, K.; Liu, C.Y.; Arnold, S.M. The unfolded protein response in nutrient sensing and differentiation. *Nature reviews Molecular cell biology* **2002**, *3*, 411-421.
20. Creighton, T.E. Protein folding coupled to disulphide bond formation. *Biological Chemistry-Hoppe Seyler* **1997**, *378*, 731-744.
21. Bergman, L.W.; Kuehl, W.M. Formation of intermolecular disulfide bonds on nascent immunoglobulin polypeptides. *Journal of Biological Chemistry* **1979**, *254*, 5690-5694.
22. Schröder, M.; Kaufman, R.J. THE MAMMALIAN UNFOLDED PROTEIN RESPONSE. *Annual Review of Biochemistry* **2005**, *74*, 739-789, doi:10.1146/annurev.biochem.73.011303.074134.
23. Schröder, M.; Clark, R.; Kaufman, R.J. IRE1- and HAC1-independent transcriptional regulation in the unfolded protein response of yeast. *Molecular Microbiology* **2003**, *49*, 591-606, doi:<https://doi.org/10.1046/j.1365-2958.2003.03585.x>.
24. Guo, J. Control of cell division by nutrients, and ER stress signaling in *Saccharomyces cerevisiae*. Texas A&M University, 2007.
25. Credle, J.J.; Finer-Moore, J.S.; Papa, F.R.; Stroud, R.M.; Walter, P. On the mechanism of sensing unfolded protein in the endoplasmic reticulum. *Proceedings of the National Academy of Sciences* **2005**, *102*, 18773-18784.
26. Zhou, J.; Liu, C.Y.; Back, S.H.; Clark, R.L.; Peisach, D.; Xu, Z.; Kaufman, R.J. The crystal structure of human IRE1 luminal domain reveals a conserved dimerization interface required for activation of the unfolded protein response. *Proceedings of the national academy of sciences* **2006**, *103*, 14343-14348.
27. Carrara, M.; Prischi, F.; Nowak, P.R.; Ali, M.M. Crystal structures reveal transient PERK luminal domain tetramerization in endoplasmic reticulum stress signaling. *The EMBO journal* **2015**, *34*, 1589-1600.
28. Shamu, C.E.; Walter, P. Oligomerization and phosphorylation of the Ire1p kinase during intracellular signaling from the endoplasmic reticulum to the nucleus. *The EMBO journal* **1996**, *15*, 3028-3039.

29. Tirasophon, W.; Welihinda, A.A.; Kaufman, R.J. A stress response pathway from the endoplasmic reticulum to the nucleus requires a novel bifunctional protein kinase/endoribonuclease (Ire1p) in mammalian cells. *Genes & development* **1998**, *12*, 1812-1824.
30. Prischi, F.; Nowak, P.; Carrara, M.; Ali, M. Phosphoregulation of Ire1 RNase splicing activity. *Nat Commun* **5**: 3554. **2014**.
31. Gardner, B.M.; Walter, P. Unfolded proteins are Ire1-activating ligands that directly induce the unfolded protein response. *Science* **2011**, *333*, 1891-1894.
32. Karagöz, G.E.; Acosta-Alvear, D.; Nguyen, H.T.; Lee, C.P.; Chu, F.; Walter, P. An unfolded protein-induced conformational switch activates mammalian IRE1. *Elife* **2017**, *6*, e30700.
33. Preissler, S.; Ron, D. Early events in the endoplasmic reticulum unfolded protein response. *Cold Spring Harbor Perspectives in Biology* **2019**, *11*, a033894.
34. Amin-Wetzel, N.; Saunders, R.A.; Kamphuis, M.J.; Rato, C.; Preissler, S.; Harding, H.P.; Ron, D. A J-protein co-chaperone recruits BiP to monomerize IRE1 and repress the unfolded protein response. *Cell* **2017**, *171*, 1625-1637. e1613.
35. Oikawa, D.; Kimata, Y.; Kohno, K.; Iwakaki, T. Activation of mammalian IRE1 $\alpha$  upon ER stress depends on dissociation of BiP rather than on direct interaction with unfolded proteins. *Experimental cell research* **2009**, *315*, 2496-2504.
36. Bertolotti, A.; Zhang, Y.; Hendershot, L.M.; Harding, H.P.; Ron, D. Dynamic interaction of BiP and ER stress transducers in the unfolded-protein response. *Nat. Cell Biol.* **2000**, *2*, 326-332.
37. Adams, C.J.; Kopp, M.C.; Larburu, N.; Nowak, P.R.; Ali, M.M. Structure and molecular mechanism of ER stress signaling by the unfolded protein response signal activator IRE1. *Frontiers in Molecular Biosciences* **2019**, *6*, 11.
38. Abravaya, K.; Myers, M.P.; Murphy, S.P.; Morimoto, R.I. The human heat shock protein hsp70 interacts with HSF, the transcription factor that regulates heat shock gene expression. *Genes & development* **1992**, *6*, 1153-1164.
39. Mayer, M.P. Hsp70 chaperone dynamics and molecular mechanism. *Trends in biochemical sciences* **2013**, *38*, 507-514.
40. Carrara, M.; Prischi, F.; Nowak, P.R.; Kopp, M.C.; Ali, M.M. Noncanonical binding of BiP ATPase domain to Ire1 and Perk is dissociated by unfolded protein CH1 to initiate ER stress signaling. *Elife* **2015**, *4*, e03522.
41. Kopp, M.C.; Nowak, P.R.; Larburu, N.; Adams, C.J.; Ali, M.M. In vitro FRET analysis of IRE1 and BiP association and dissociation upon endoplasmic reticulum stress. *Elife* **2018**, *7*, e30257.
42. Sepulveda, D.; Rojas-Rivera, D.; Rodriguez, D.A.; Groenendyk, J.; Köhler, A.; Lebeaupin, C.; Ito, S.; Urra, H.; Carreras-Sureda, A.; Hazari, Y. Interactome screening identifies the ER luminal chaperone Hsp47 as a regulator of the unfolded protein response transducer IRE1 $\alpha$ . *Molecular cell* **2018**, *69*, 238-252. e237.
43. Todd-Corlett, A.; Jones, E.; Seghers, C.; Gething, M.-J. Lobe IB of the ATPase domain of Kar2p/BiP interacts with Ire1p to negatively regulate the unfolded protein response in *Saccharomyces cerevisiae*. *Journal of molecular biology* **2007**, *367*, 770-787.
44. Craig, E.A. Hsp70 at the membrane: driving protein translocation. *BMC biology* **2018**, *16*, 1-11.
45. Krimmer, T.; Rassow, J.; Kunau, W.-H.; Voos, W.; Pfanner, N. Mitochondrial protein import motor: the ATPase domain of matrix Hsp70 is crucial for binding to Tim44, while the peptide binding domain and the carboxy-terminal segment play a stimulatory role. *Molecular and cellular biology* **2000**, *20*, 5879-5887.
46. Liu, Q.; D'Silva, P.; Walter, W.; Marszalek, J.; Craig, E.A. Regulated cycling of mitochondrial Hsp70 at the protein import channel. *Science* **2003**, *300*, 139-141.
47. Snapp, E.L. Unfolded protein responses with or without unfolded proteins? *cells* **2012**, *1*, 926-950.

48. Kimata, Y.; Ishiwata-Kimata, Y.; Ito, T.; Hirata, A.; Suzuki, T.; Oikawa, D.; Takeuchi, M.; Kohno, K. Two regulatory steps of ER-stress sensor Ire1 involving its cluster formation and interaction with unfolded proteins. *Journal of Cell Biology* **2007**, *179*, 75-86.
49. Armstrong, M.C.; Šestak, S.; Ali, A.A.; Sagini, H.A.; Brown, M.; Baty, K.; Treumann, A.; Schröder, M. Bypass of activation loop phosphorylation by aspartate 836 in activation of the endoribonuclease activity of Ire1. *Molecular and Cellular Biology* **2017**, *37*.
50. Lee, K.P.; Dey, M.; Neculai, D.; Cao, C.; Dever, T.E.; Sicheri, F. Structure of the dual enzyme Ire1 reveals the basis for catalysis and regulation in nonconventional RNA splicing. *Cell* **2008**, *132*, 89-100.
51. Cao, S.S.; Kaufman, R.J. Unfolded protein response. *Current biology* **2012**, *22*, R622-R626.
52. Nojima, H.; Leem, S.-H.; Araki, H.; Sakai, A.; Nakashima, N.; Kanaoka, Y.; Ono, Y. Hac1: A novel yeast bZIP protein binding to the CRE motif is a multicopy suppressor for cdcW mutant of *Schizosaccharomyces pombe*. *Nucleic acids research* **1994**, *22*, 5279-5288.
53. Nikawa, J.-i.; Akiyoshi, M.; Hirata, S.; Fukuda, T. *Saccharomyces cerevisiae* IRE2/HAC1 is involved in IRE1-mediated KAR2 expression. *Nucleic acids research* **1996**, *24*, 4222-4226.
54. Cox, J.S.; Walter, P. A novel mechanism for regulating activity of a transcription factor that controls the unfolded protein response. *Cell* **1996**, *87*, 391-404.
55. Schröder, M.; Kaufman, R.J. ER stress and the unfolded protein response. *Mutation Research/Fundamental and Molecular Mechanisms of Mutagenesis* **2005**, *569*, 29-63.
56. Kawahara, T.; Yanagi, H.; Yura, T.; Mori, K. Endoplasmic reticulum stress-induced mRNA splicing permits synthesis of transcription factor Hac1p/Ern4p that activates the unfolded protein response. *Molecular biology of the cell* **1997**, *8*, 1845-1862.
57. Gonzalez, T.N.; Sidrauski, C.; Dörfler, S.; Walter, P. Mechanism of non-spliceosomal mRNA splicing in the unfolded protein response pathway. *The EMBO journal* **1999**, *18*, 3119-3132.
58. Schindler, A.J.; Schekman, R. In vitro reconstitution of ER-stress induced ATF6 transport in COPII vesicles. *Proceedings of the National Academy of Sciences* **2009**, *106*, 17775-17780.
59. Haze, K.; Yoshida, H.; Yanagi, H.; Yura, T.; Mori, K. Mammalian transcription factor ATF6 is synthesized as a transmembrane protein and activated by proteolysis in response to endoplasmic reticulum stress. *Molecular biology of the cell* **1999**, *10*, 3787-3799.
60. Ye, J.; Rawson, R.B.; Komuro, R.; Chen, X.; Davé, U.P.; Prywes, R.; Brown, M.S.; Goldstein, J.L. ER stress induces cleavage of membrane-bound ATF6 by the same proteases that process SREBPs. *Molecular cell* **2000**, *6*, 1355-1364.
61. Brown, M.S.; Ye, J.; Rawson, R.B.; Goldstein, J.L. Regulated intramembrane proteolysis: a control mechanism conserved from bacteria to humans. *Cell* **2000**, *100*, 391-398.
62. Brown, M.S.; Goldstein, J.L. The SREBP pathway: regulation of cholesterol metabolism by proteolysis of a membrane-bound transcription factor. *Cell* **1997**, *89*, 331-340.
63. Nohturfft, A.; Yabe, D.; Goldstein, J.L.; Brown, M.S.; Espenshade, P.J. Regulated step in cholesterol feedback localized to budding of SCAP from ER membranes. *Cell* **2000**, *102*, 315-323.
64. Sakai, J.; Nohturfft, A.; Goldstein, J.L.; Brown, M.S. Cleavage of sterol regulatory element-binding proteins (SREBPs) at site-1 requires interaction with SREBP cleavage-activating protein: evidence from in vivo competition studies. *Journal of Biological Chemistry* **1998**, *273*, 5785-5793.
65. Duncan, E.A.; Brown, M.S.; Goldstein, J.L.; Sakai, J. Cleavage site for sterol-regulated protease localized to a Leu-Ser bond in the lumenal loop of sterol regulatory element-binding protein-2. *Journal of Biological Chemistry* **1997**, *272*, 12778-12785.
66. Liu, C.Y.; Schröder, M.; Kaufman, R.J. Ligand-independent Dimerization Activates the Stress Response Kinases IRE1 and PERK in the Lumen of the Endoplasmic Reticulum\*. *Journal of Biological Chemistry* **2000**, *275*, 24881-24885, doi:<https://doi.org/10.1074/jbc.M004454200>.

67. Liu, C.Y.; Xu, Z.; Kaufman, R.J. Structure and Intermolecular Interactions of the Luminal Dimerization Domain of Human IRE1 $\alpha$ \*. *Journal of Biological Chemistry* **2003**, *278*, 17680-17687, doi:<https://doi.org/10.1074/jbc.M300418200>.
68. Harding, H.P.; Zhang, Y.; Ron, D. Protein translation and folding are coupled by an endoplasmic-reticulum-resident kinase. *Nature* **1999**, *397*, 271-274.
69. Ma, K.; Vattem, K.M.; Wek, R.C. Dimerization and Release of Molecular Chaperone Inhibition Facilitate Activation of Eukaryotic Initiation Factor-2 Kinase in Response to Endoplasmic Reticulum Stress\*. *Journal of Biological Chemistry* **2002**, *277*, 18728-18735, doi:<https://doi.org/10.1074/jbc.M200903200>.
70. Vattem, K.M.; Wek, R.C. Reinitiation involving upstream ORFs regulates  $\text{ATF4}$  mRNA translation in mammalian cells. *Proceedings of the National Academy of Sciences of the United States of America* **2004**, *101*, 11269-11274, doi:10.1073/pnas.0400541101.
71. Harding, H.P.; Novoa, I.; Zhang, Y.; Zeng, H.; Wek, R.; Schapira, M.; Ron, D. Regulated Translation Initiation Controls Stress-Induced Gene Expression in Mammalian Cells. *Molecular Cell* **2000**, *6*, 1099-1108, doi:[https://doi.org/10.1016/S1097-2765\(00\)00108-8](https://doi.org/10.1016/S1097-2765(00)00108-8).
72. Jiang, H.-Y.; Wek, S.A.; McGrath, B.C.; Lu, D.; Hai, T.; Harding, H.P.; Wang, X.; Ron, D.; Cavener, D.R.; Wek, R.C. Activating Transcription Factor 3 Is Integral to the Eukaryotic Initiation Factor 2 Kinase Stress Response. *Molecular and Cellular Biology* **2004**, *24*, 1365-1377, doi:10.1128/mcb.24.3.1365-1377.2004.
73. Nolen, B.; Taylor, S.; Ghosh, G. Regulation of protein kinases: controlling activity through activation segment conformation. *Molecular cell* **2004**, *15*, 661-675.
74. Welihinda, A.A.; Kaufman, R.J. The unfolded protein response pathway in *Saccharomyces cerevisiae*: oligomerization and trans-phosphorylation of Ire1p (Ern1p) are required for kinase activation. *Journal of Biological Chemistry* **1996**, *271*, 18181-18187.
75. Korennykh, A.V.; Egea, P.F.; Korostelev, A.A.; Finer-Moore, J.; Zhang, C.; Shokat, K.M.; Stroud, R.M.; Walter, P. The unfolded protein response signals through high-order assembly of Ire1. *Nature* **2009**, *457*, 687-693.
76. Mannan, M.A.-u.; Shadrack, W.R.; Biener, G.; Shin, B.-S.; Anshu, A.; Raicu, V.; Frick, D.N.; Dey, M. An Ire1–Phk1 Chimera Reveals a Dispensable Role of Autokinase Activity in Endoplasmic Reticulum Stress Response. *Journal of molecular biology* **2013**, *425*, 2083-2099.
77. Papa, F.R.; Zhang, C.; Shokat, K.; Walter, P. Bypassing a kinase activity with an ATP-competitive drug. *Science* **2003**, *302*, 1533-1537.
78. Korennykh, A.V.; Egea, P.F.; Korostelev, A.A.; Finer-Moore, J.; Stroud, R.M.; Zhang, C.; Shokat, K.M.; Walter, P. Cofactor-mediated conformational control in the bifunctional kinase/RNase Ire1. *BMC biology* **2011**, *9*, 1-16.
79. Chawla, A.; Chakrabarti, S.; Ghosh, G.; Niwa, M. Attenuation of yeast UPR is essential for survival and is mediated by IRE1 kinase. *Journal of Cell Biology* **2011**, *193*, 41-50.
80. Rubio, C.; Pincus, D.; Korennykh, A.; Schuck, S.; El-Samad, H.; Walter, P. Homeostatic adaptation to endoplasmic reticulum stress depends on Ire1 kinase activity. *Journal of Cell Biology* **2011**, *193*, 171-184.
81. Mori, K.; Kawahara, T.; Yoshida, H.; Yanagi, H.; Yura, T. Signalling from endoplasmic reticulum to nucleus: transcription factor with a basic-leucine zipper motif is required for the unfolded protein-response pathway. *Genes to Cells* **1996**, *1*, 803-817.
82. Welihinda, A.A.; Tirasophon, W.; Kaufman, R.J. The cellular response to protein misfolding in the endoplasmic reticulum. *Gene Expression The Journal of Liver Research* **1999**, *7*, 293-300.
83. Kuhn, K.M.; DeRisi, J.L.; Brown, P.O.; Sarnow, P. Global and specific translational regulation in the genomic response of *Saccharomyces cerevisiae* to a rapid transfer from a fermentable to a nonfermentable carbon source. *Molecular and cellular biology* **2001**, *21*, 916-927.
84. Payne, T.; Hanfrey, C.; Bishop, A.L.; Michael, A.J.; Avery, S.V.; Archer, D.B. Transcript-specific translational regulation in the unfolded protein response of *Saccharomyces cerevisiae*. *FEBS letters* **2008**, *582*, 503-509.

85. Xia, X. Translation Control of HAC1 by Regulation of Splicing in *Saccharomyces cerevisiae*. *International journal of molecular sciences* **2019**, *20*, 2860.
86. Mori, K.; Ogawa, N.; Kawahara, T.; Yanagi, H.; Yura, T. mRNA splicing-mediated C-terminal replacement of transcription factor Hac1p is required for efficient activation of the unfolded protein response. *Proceedings of the National Academy of Sciences* **2000**, *97*, 4660-4665.
87. Chapman, R.E.; Walter, P. Translational attenuation mediated by an mRNA intron. *Current Biology* **1997**, *7*, 850-859.
88. Pal, B.; Chan, N.C.; Helfenbaum, L.; Tan, K.; Tansey, W.P.; Gething, M.-J. SCFCdc4-mediated degradation of the Hac1p transcription factor regulates the unfolded protein response in *Saccharomyces cerevisiae*. *Molecular biology of the cell* **2007**, *18*, 426-440.
89. Ogawa, N.; Mori, K. Autoregulation of the HAC1 gene is required for sustained activation of the yeast unfolded protein response. *Genes to Cells* **2004**, *9*, 95-104.
90. Mori, K.; Sant, A.; Kohno, K.; Normington, K.; Gething, M.; Sambrook, J. A 22 bp cis-acting element is necessary and sufficient for the induction of the yeast KAR2 (BiP) gene by unfolded proteins. *The EMBO journal* **1992**, *11*, 2583-2593.
91. Yoshida, H.; Haze, K.; Yanagi, H.; Yura, T.; Mori, K. Identification of the cis-acting endoplasmic reticulum stress response element responsible for transcriptional induction of mammalian glucose-regulated proteins: involvement of basic leucine zipper transcription factors. *Journal of Biological Chemistry* **1998**, *273*, 33741-33749.
92. Spode, I.; Maiwald, D.; Hollenberg, C.P.; Suckow, M. ATF/CREB sites present in sub-telomeric regions of *Saccharomyces cerevisiae* chromosomes are part of promoters and act as UAS/URS of highly conserved COS genes. *Journal of molecular biology* **2002**, *319*, 407-420.
93. Schröder, M.; Clark, R.; Liu, C.Y.; Kaufman, R.J. The unfolded protein response represses differentiation through the RPD3-SIN3 histone deacetylase. *The EMBO journal* **2004**, *23*, 2281-2292.
94. Gething, M.-J. Role and regulation of the ER chaperone BiP. In *Proceedings of the Seminars in cell & developmental biology*, 1999; pp. 465-472.
95. Blond-Elguindi, S.; Fourie, A.; Sambrook, J.; Gething, M. Peptide-dependent stimulation of the ATPase activity of the molecular chaperone BiP is the result of conversion of oligomers to active monomers. *Journal of Biological Chemistry* **1993**, *268*, 12730-12735.
96. Ledford, B.E.; Leno, G.H. ADP-ribosylation of the molecular chaperone GRP78/BiP. *Molecular and cellular biochemistry* **1994**, *138*, 141-148.
97. Freiden, P.J.; Gaut, J.; Hendershot, L. Interconversion of three differentially modified and assembled forms of BiP. *The EMBO journal* **1992**, *11*, 63-70.
98. Hwang, J.; Qi, L. Quality control in the endoplasmic reticulum: crosstalk between ERAD and UPR pathways. *Trends in biochemical sciences* **2018**, *43*, 593-605.
99. Theo van, L.; Alex, J.v.d.E.; Carrol, T. Mif1: A Missing Link between the Unfolded Protein Response Pathway and ER-Associated Protein Degradation? *Current Protein & Peptide Science* **2001**, *2*, 169-190, doi:<http://dx.doi.org/10.2174/1389203013381189>.
100. Wu, S.; Stone, S.; Nave, K.-A.; Lin, W. The Integrated UPR and ERAD in Oligodendrocytes Maintain Myelin Thickness in Adults by Regulating Myelin Protein Translation. *Journal of Neuroscience* **2020**, *40*, 8214-8232.
101. Hori, O.; Ichinoda, F.; Yamaguchi, A.; Tamatani, T.; Taniguchi, M.; Koyama, Y.; Katayama, T.; Tohyama, M.; Stern, D.M.; Ozawa, K.; et al. Role of Herp in the endoplasmic reticulum stress response. *Genes to Cells* **2004**, *9*, 457-469, doi:<https://doi.org/10.1111/j.1356-9597.2004.00735.x>.
102. Hosokawa, N.; Tremblay, L.O.; You, Z.; Herscovics, A.; Wada, I.; Nagata, K. Enhancement of Endoplasmic Reticulum (ER) Degradation of Misfolded Null Hong Kong  $\alpha$ 1-Antitrypsin by Human ER Mannosidase I\*. *Journal of Biological Chemistry* **2003**, *278*, 26287-26294, doi:<https://doi.org/10.1074/jbc.M303395200>.

103. Yoshida, H.; Matsui, T.; Hosokawa, N.; Kaufman, R.J.; Nagata, K.; Mori, K. A Time-Dependent Phase Shift in the Mammalian Unfolded Protein Response. *Developmental Cell* **2003**, *4*, 265-271, doi:[https://doi.org/10.1016/S1534-5807\(03\)00022-4](https://doi.org/10.1016/S1534-5807(03)00022-4).
104. Qu, J.; Zou, T.; Lin, Z. The Roles of the Ubiquitin–Proteasome System in the Endoplasmic Reticulum Stress Pathway. *International Journal of Molecular Sciences* **2021**, *22*, 1526.
105. Johnson, L.N.; Noble, M.E.; Owen, D.J. Active and inactive protein kinases: structural basis for regulation. *Cell* **1996**, *85*, 149-158.
106. Manning, G.; Whyte, D.B.; Martinez, R.; Hunter, T.; Sudarsanam, S. The protein kinase complement of the human genome. *Science* **2002**, *298*, 1912-1934.
107. Knighton, D.R.; Zheng, J.H.; Ten Eyck, L.F.; Ashford, V.A.; Xuong, N.-H.; Taylor, S.S.; Sowadski, J.M. Crystal structure of the catalytic subunit of cyclic adenosine monophosphate-dependent protein kinase. *Science* **1991**, *253*, 407-414.
108. Goldberg, J.; Nairn, A.C.; Kuriyan, J. Structural basis for the autoinhibition of calcium/calmodulin-dependent protein kinase I. *Cell* **1996**, *84*, 875-887.
109. De Bondt, H.L.; Rosenblatt, J.; Jancarik, J.; Jones, H.D.; Morgant, D.O.; Kim, S.-H. Crystal structure of cyclin-dependent kinase 2. *Nature* **1993**, *363*, 595-602.
110. Skamnaki, V.; Owen, D.; Noble, M.; Lowe, E.; Lowe, G.; Oikonomakos, N.; Johnson, L. Catalytic mechanism of phosphorylase kinase probed by mutational studies. *Biochemistry* **1999**, *38*, 14718-14730.
111. Leon, B.C.; Tsigelny, I.; Adams, J.A. Electrostatic environment surrounding the activation loop phosphotyrosine in the oncoprotein v-Fps. *Biochemistry* **2001**, *40*, 10078-10086.
112. Cox, J.S.; Chapman, R.E.; Walter, P. The unfolded protein response coordinates the production of endoplasmic reticulum protein and endoplasmic reticulum membrane. *Molecular biology of the cell* **1997**, *8*, 1805-1814.
113. Stroobants, A.K.; Hettema, E.H.; van den Berg, M.; Tabak, H.F. Enlargement of the endoplasmic reticulum membrane in *Saccharomyces cerevisiae* is not necessarily linked to the unfolded protein response via Ire1p. *FEBS letters* **1999**, *453*, 210-214.
114. Chang, H.J.; Jones, E.W.; Henry, S.A. Role of the unfolded protein response pathway in regulation of INO1 and in the sec14 bypass mechanism in *Saccharomyces cerevisiae*. *Genetics* **2002**, *162*, 29-43.
115. Loewen, C.; Gaspar, M.; Jesch, S.; Delon, C.; Ktistakis, N.; Henry, S.; Levine, T. Phospholipid metabolism regulated by a transcription factor sensing phosphatidic acid. *Science* **2004**, *304*, 1644-1647.
116. Schröder, M.; Chang, J.S.; Kaufman, R.J. The unfolded protein response represses nitrogen-starvation induced developmental differentiation in yeast. *Genes & development* **2000**, *14*, 2962-2975.
117. Zong, W.-X.; Li, C.; Hatzivassiliou, G.; Lindsten, T.; Yu, Q.-C.; Yuan, J.; Thompson, C.B. Bax and Bak can localize to the endoplasmic reticulum to initiate apoptosis. *The Journal of cell biology* **2003**, *162*, 59-69.
118. Scorrano, L.; Oakes, S.A.; Opferman, J.T.; Cheng, E.H.; Sorcinelli, M.D.; Pozzan, T.; Korsmeyer, S.J. BAX and BAK regulation of endoplasmic reticulum Ca<sup>2+</sup>: a control point for apoptosis. *Science* **2003**, *300*, 135-139.
119. Nakagawa, T.; Yuan, J. Cross-talk between two cysteine protease families: activation of caspase-12 by calpain in apoptosis. *The Journal of cell biology* **2000**, *150*, 887-894.
120. Gibson, B.W.; Bredesen, D.E.; Rao, R.V.; Poksay, K.S.; Castro-Obregon, S.; Schilling, B.; Row, R.H.; del Rio, G.; Ellerby, H.M. Molecular components of a cell death pathway activated by endoplasmic reticulum stress. *Journal of Biological Chemistry* **2004**, *279*, 177-187.
121. Crompton, M. The mitochondrial permeability transition pore and its role in cell death. *Biochemical Journal* **1999**, *341*, 233-249.
122. Nishitoh, H.; Matsuzawa, A.; Tobiume, K.; Saegusa, K.; Takeda, K.; Inoue, K.; Hori, S.; Kakizuka, A.; Ichijo, H. ASK1 is essential for endoplasmic reticulum stress-induced neuronal

- cell death triggered by expanded polyglutamine repeats. *Genes & development* **2002**, *16*, 1345-1355.
123. Yoneda, T.; Imaizumi, K.; Oono, K.; Yui, D.; Gomi, F.; Katayama, T.; Tohyama, M. Activation of caspase-12, an endoplasmic reticulum (ER) resident caspase, through tumor necrosis factor receptor-associated factor 2-dependent mechanism in response to the ER stress. *Journal of Biological Chemistry* **2001**, *276*, 13935-13940.
  124. Chen, Z.; Cole, P.A. Synthetic approaches to protein phosphorylation. *Current opinion in chemical biology* **2015**, *28*, 115-122, doi:10.1016/j.cbpa.2015.07.001.
  125. Kuo, S.C.; Lampen, J.O. Tunicamycin inhibition of [<sup>3</sup>H]glucosamine incorporation into yeast glycoproteins: Binding of tunicamycin and interaction with phospholipids. *Archives of biochemistry and biophysics* **1976**, *172*, 574-581, doi:10.1016/0003-9861(76)90110-7.
  126. Leavitt, R.; Schlesinger, S.; Kornfeld, S. Tunicamycin inhibits glycosylation and multiplication of Sindbis and vesicular stomatitis viruses. *The Journal of Virology* **1977**, *21*, 375, doi:10.1128/JVI.21.1.375-385.1977.
  127. Messias Sandes, J.; Nascimento Moura, D.M.; Divina Da Silva Santiago, M.; Barbosa de Lima, G.; Cabral Filho, P.E.; Da Cunha Gonçalves de Albuquerque, S.; de Paiva Cavalcanti, M.; Fontes, A.; Bressan Queiroz Figueiredo, R.C. The effects of endoplasmic reticulum stressors, tunicamycin and dithiothreitol on *Trypanosoma cruzi*. *Experimental cell research* **2019**, *383*, doi:10.1016/j.yexcr.2019.111560.
  128. Guo, J.; Polymenis, M. Dcr2 targets Ire1 and downregulates the unfolded protein response in *Saccharomyces cerevisiae*. *EMBO reports* **2006**, *7*, 1124-1127.
  129. Pathak, R.; Bogomolnaya, L.M.; Guo, J.; Polymenis, M. Gid8p (Dcr1p) and Dcr2p function in a common pathway to promote START completion in *Saccharomyces cerevisiae*. *Eukaryotic Cell* **2004**, *3*, 1627-1638.
  130. Spellman, P.T.; Sherlock, G.; Zhang, M.Q.; Iyer, V.R.; Anders, K.; Eisen, M.B.; Brown, P.O.; Botstein, D.; Futcher, B. Comprehensive identification of cell cycle-regulated genes of the yeast *Saccharomyces cerevisiae* by microarray hybridization. *Molecular biology of the cell* **1998**, *9*, 3273-3297.
  131. Mertz, P.; Yu, L.; Sikkink, R.; Rusnak, F. Kinetic and spectroscopic analyses of mutants of a conserved histidine in the metallophosphatases calcineurin and  $\lambda$  protein phosphatase. *Journal of Biological Chemistry* **1997**, *272*, 21296-21302.
  132. Zhuo, S.; Clemens, J.C.; Stone, R.L.; Dixon, J.E. Mutational analysis of a Ser/Thr phosphatase. Identification of residues important in phosphoesterase substrate binding and catalysis. *Journal of Biological Chemistry* **1994**, *269*, 26234-26238.
  133. Welihinda, A.A.; Tirasophon, W.; Green, S.R.; Kaufman, R.J. Protein Serine/Threonine Phosphatase Ptc2p Negatively Regulates the Unfolded-Protein Response by Dephosphorylating Ire1p Kinase. *Molecular and Cellular Biology* **1998**, *18*, 1967-1977, doi:doi:10.1128/MCB.18.4.1967.
  134. Aragón, T.; Van Anken, E.; Pincus, D.; Serafimova, I.M.; Korennykh, A.V.; Rubio, C.A.; Walter, P. Messenger RNA targeting to endoplasmic reticulum stress signalling sites. *Nature* **2009**, *457*, 736-740.
  135. Prinz, W.A.; Grzyb, L.; Veenhuis, M.; Kahana, J.A.; Silver, P.A.; Rapoport, T.A. Mutants affecting the structure of the cortical endoplasmic reticulum in *Saccharomyces cerevisiae*. *The Journal of cell biology* **2000**, *150*, 461-474.
  136. Chee, M.K.; Haase, S.B. New and redesigned pRS plasmid shuttle vectors for genetic manipulation of *Saccharomyces cerevisiae*. *G3: Genes/ Genomes/ Genetics* **2012**, *2*, 515-526.
  137. Voytas, D. Agarose gel electrophoresis. *Current protocols in immunology* **1992**, *2*, 10.14. 11-10.14. 18.
  138. Gietz, R.D.; Schiestl, R.H. High-efficiency yeast transformation using the LiAc/SS carrier DNA/PEG method. *Nature protocols* **2007**, *2*, 31-34.

139. Osowski, C.M.; Urano, F. Measuring ER stress and the unfolded protein response using mammalian tissue culture system. In *Methods in enzymology*; Elsevier: 2011; Volume 490, pp. 71-92.
140. Cox, J.S.; Shamu, C.E.; Walter, P. Transcriptional induction of genes encoding endoplasmic reticulum resident proteins requires a transmembrane protein kinase. *Cell* **1993**, *73*, 1197-1206.
141. Kohno, K.; Normington, K.; Sambrook, J.; Gething, M.; Mori, K. The promoter region of the yeast KAR2 (BiP) gene contains a regulatory domain that responds to the presence of unfolded proteins in the endoplasmic reticulum. *Molecular and cellular biology* **1993**, *13*, 877-890.
142. Pincus, D.; Chevalier, M.W.; Aragón, T.; Van Anken, E.; Vidal, S.E.; El-Samad, H.; Walter, P. BiP binding to the ER-stress sensor Ire1 tunes the homeostatic behavior of the unfolded protein response. *PLoS biology* **2010**, *8*, e1000415.
143. Kinoshita, E.; Kinoshita-Kikuta, E.; Koike, T. Separation and detection of large phosphoproteins using Phos-tag SDS-PAGE. *Nature protocols* **2009**, *4*, 1513-1521.